EndoTOFPET-US: A multi-modal endoscope for Ultrasound and Time-of-Flight PET

Marco Pizzichemi
On behalf of the EndoTOFPET-US collaboration

International Medical Physics and Biomedical Engineering Workshop
Ohrid, Macedonia, July 25-28 2018

Outline

- Introduction
- Motivations
- Technological challenges
- Detector design
- Performance of individual sub-detectors
- Conclusions

Introduction

The EndoTOFPET-US project

➔ International collaboration in the frame of the **European FP7 program**

- ➢ 7 academic partners: CERN, DESY, LIP, TU-Delft, TUM, Heidelberg Uni, Milano-Bicocca Uni
- ➢ 3 industrial partners: KLOE, Fibercryst, Surgiceye
- ➢ 3 clinical partners: Aix-Marseille Uni, Klinikum Recht der Isar-TU Munich, Lausanne Uni

The EndoTOFPET-US project

- International collaboration in the frame of the **European FP7 program**
  - 7 academic partners: CERN, DESY, LIP, TU-Delft, TUM, Heidelberg Uni, Milano-Bicocca Uni
  - 3 industrial partners: KLOE, Fibercryst, Surgiceye
  - 3 clinical partners: Aix-Marseille Uni, Klinikum Recht der Isar-TU Munich, Lausanne Uni
- Develop an imaging tool for early diagnosis of **pancreas** and **prostate** cancer

The EndoTOFPET-US project

Endoscopic Probe

- US detector
- PET head

External PET Plate

➔ International collaboration in the frame of the **European FP7 program**

- ➢ 7 academic partners: CERN, DESY, LIP, TU-Delft, TUM, Heidelberg Uni, Milano-Bicocca Uni
- ➢ 3 industrial partners: KLOE, Fibercryst, Surgiceye
- ➢ 3 clinical partners: Aix-Marseille Uni, Klinikum Recht der Isar-TU Munich, Lausanne Uni

➔ Develop an imaging tool for early diagnosis of **pancreas** and **prostate** cancer

➔ Combine a **high resolution PET scanner** with an endoscopic **US probe**

The EndoTOFPET-US project

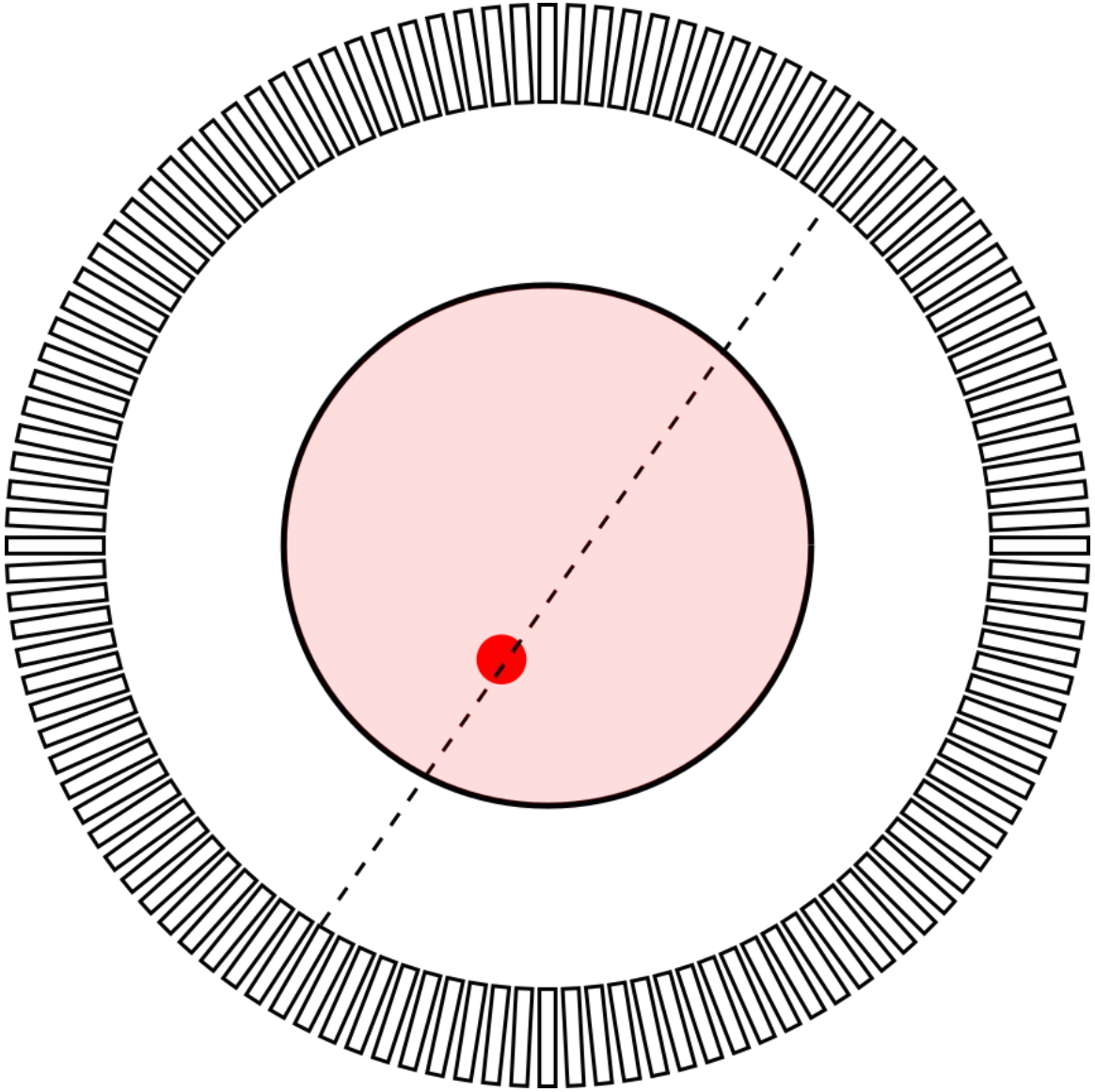

The EndoTOFPET-US project

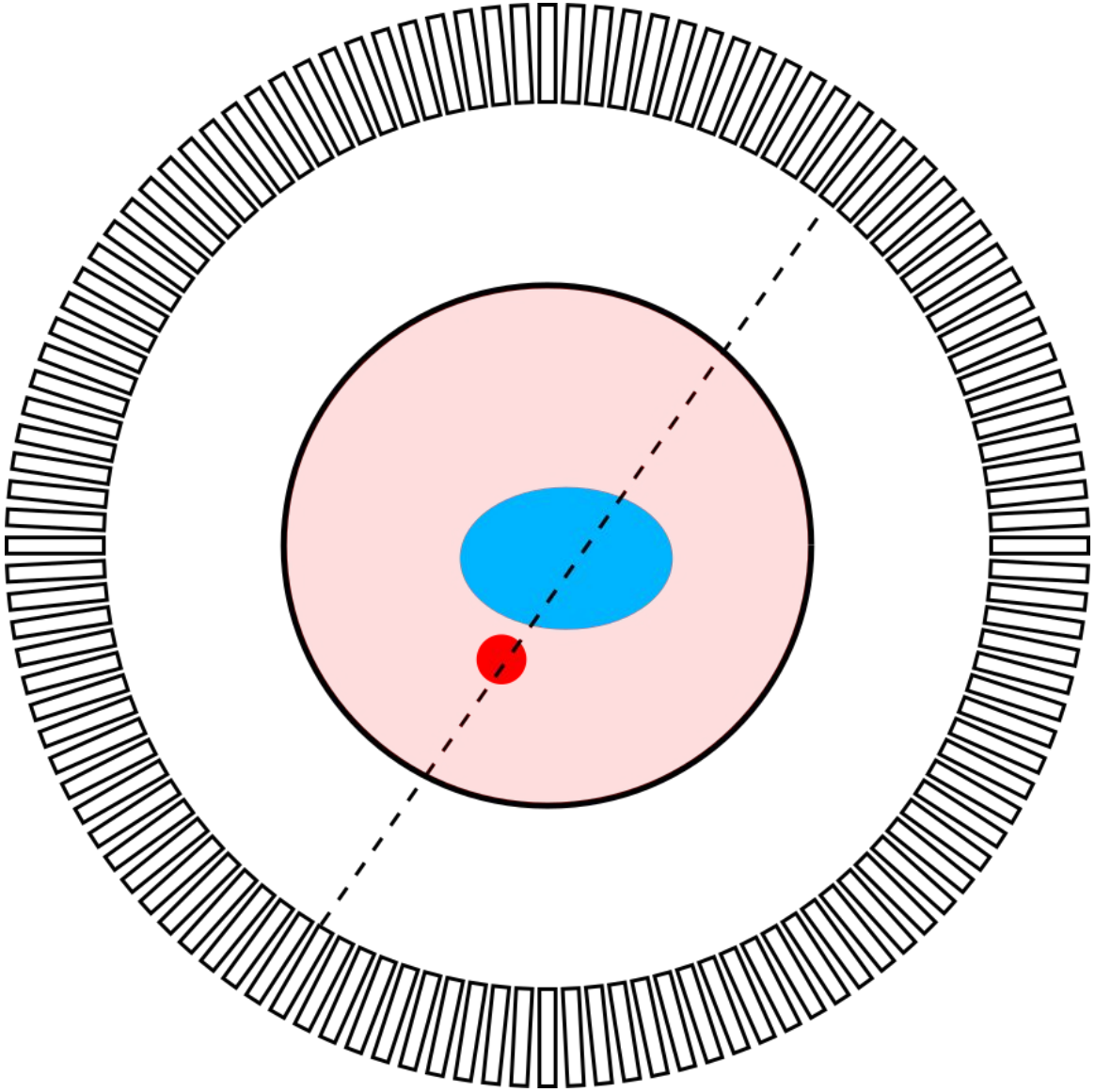

The EndoTOFPET-US project

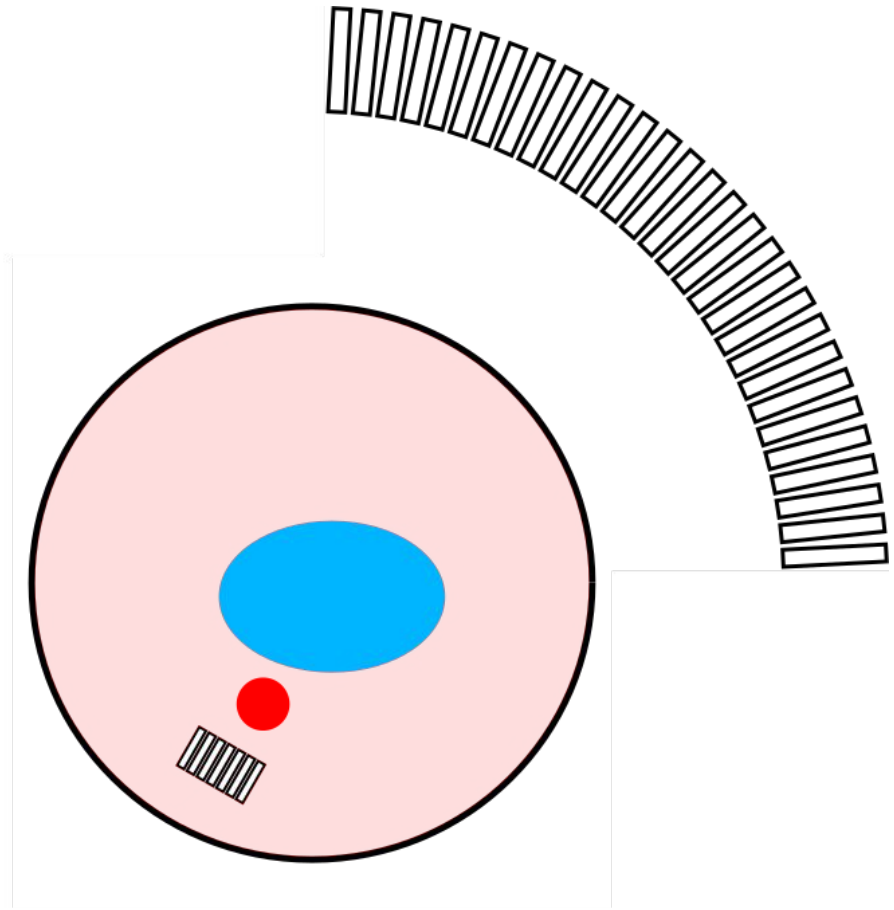

Motivation

Pancreas and prostate cancers

Pancreatic Cancer

Pancreas and prostate cancers

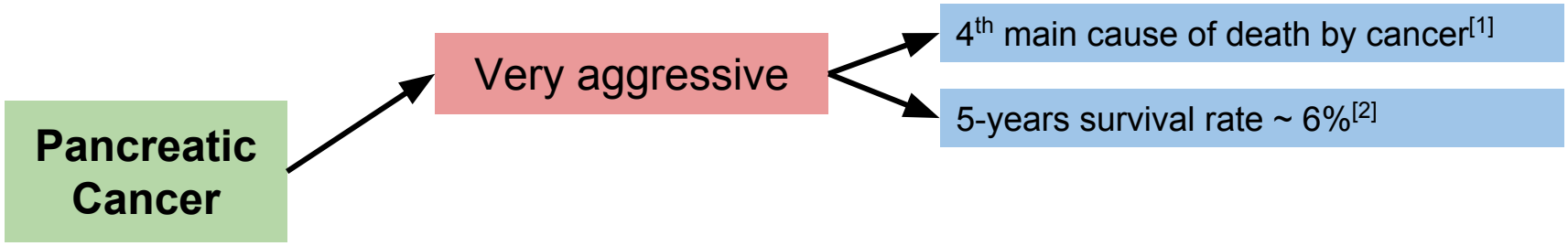

[1] Jemal A, Siegel R, Ward E et al. (2008). "Cancer statistics, 2008". CA Cancer J Clin 58 (2): 71–96.

[2] American Cancer Society (2010). "Cancer Facts and Figures 2010"

Pancreas and prostate cancers

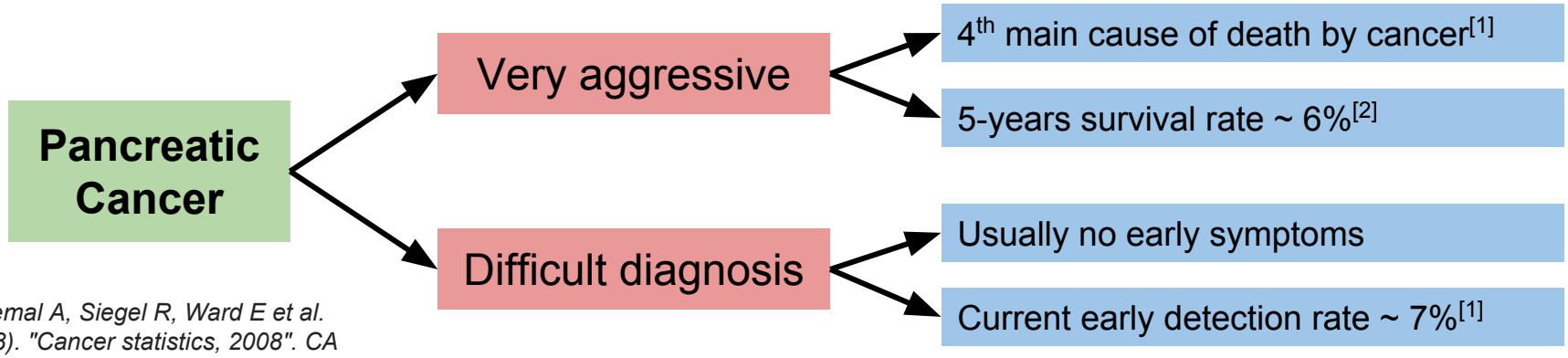

[1] Jemal A, Siegel R, Ward E et al. (2008). "Cancer statistics, 2008". CA Cancer J Clin 58 (2): 71–96.

[2] American Cancer Society (2010). "Cancer Facts and Figures 2010"

Pancreas and prostate cancers

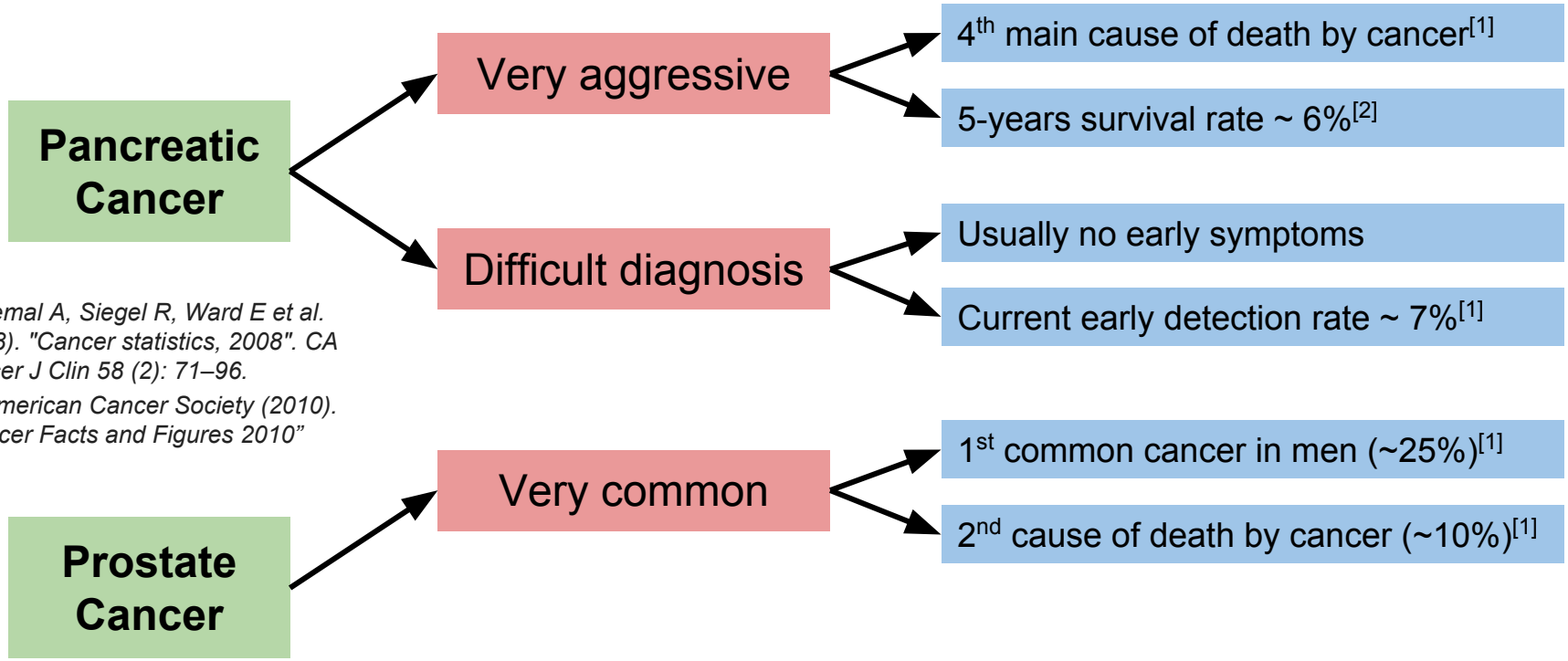

[1] Jemal A, Siegel R, Ward E et al. (2008). "Cancer statistics, 2008". CA Cancer J Clin 58 (2): 71–96.

[2] American Cancer Society (2010). "Cancer Facts and Figures 2010"

Pancreas and prostate cancers

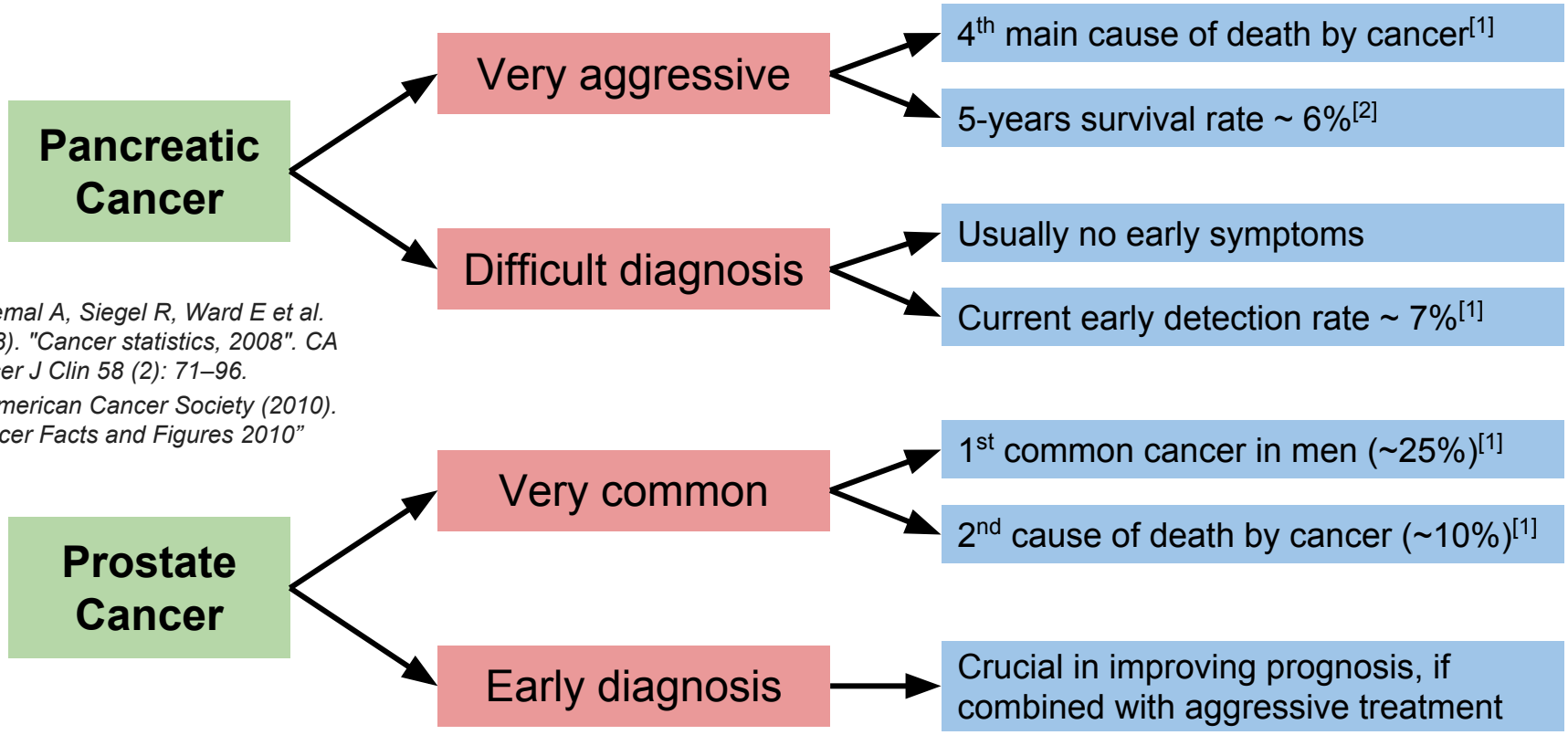

[1] Jemal A, Siegel R, Ward E et al. (2008). "Cancer statistics, 2008". CA Cancer J Clin 58 (2): 71–96.

[2] American Cancer Society (2010). "Cancer Facts and Figures 2010"

Pancreas and prostate cancers

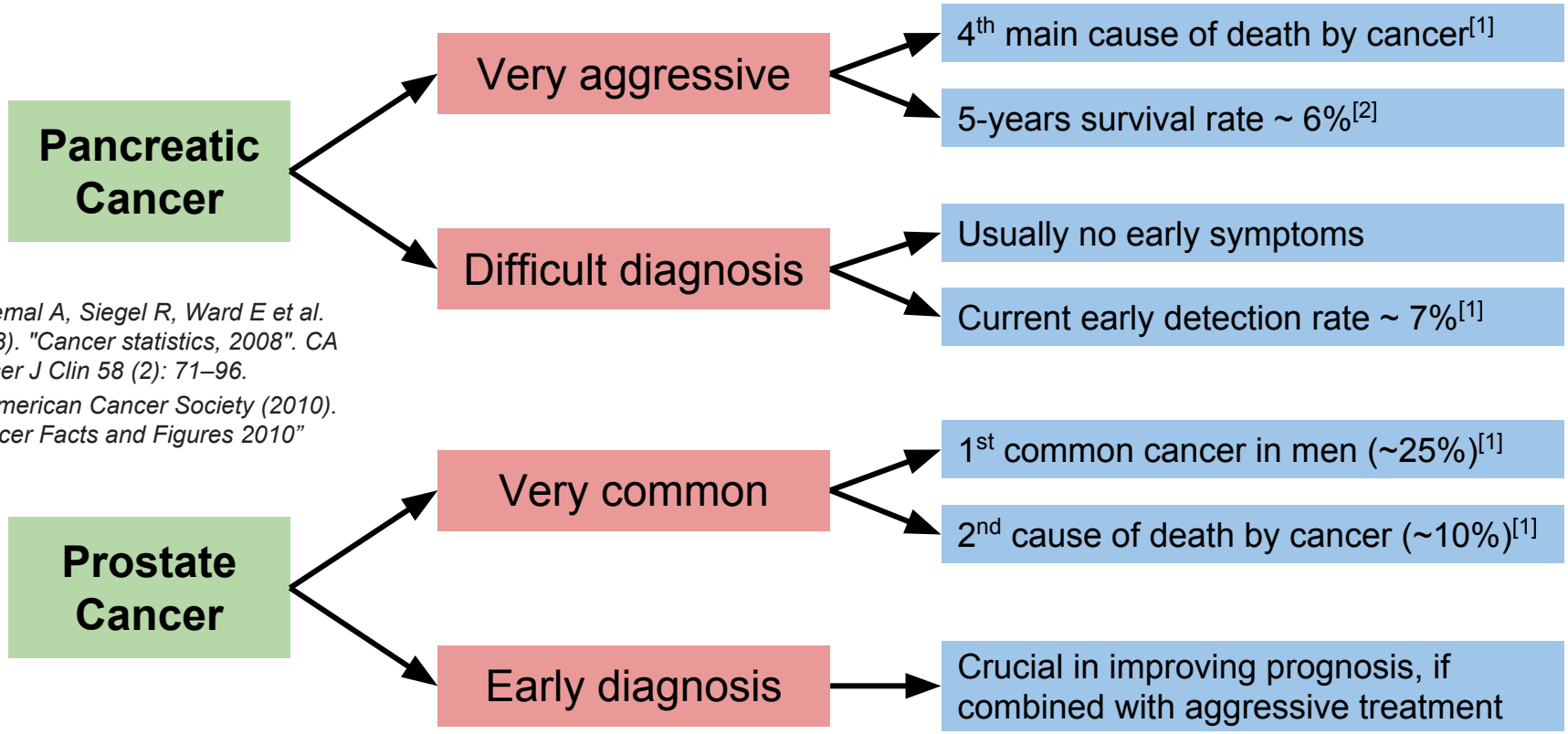

[1] Jemal A, Siegel R, Ward E et al. (2008). "Cancer statistics, 2008". CA Cancer J Clin 58 (2): 71–96.

[2] American Cancer Society (2010). "Cancer Facts and Figures 2010"

➔ Standard imaging nowadays performed with **US**, **CT** and **MRI,** not **PET**

Pancreas and prostate cancers

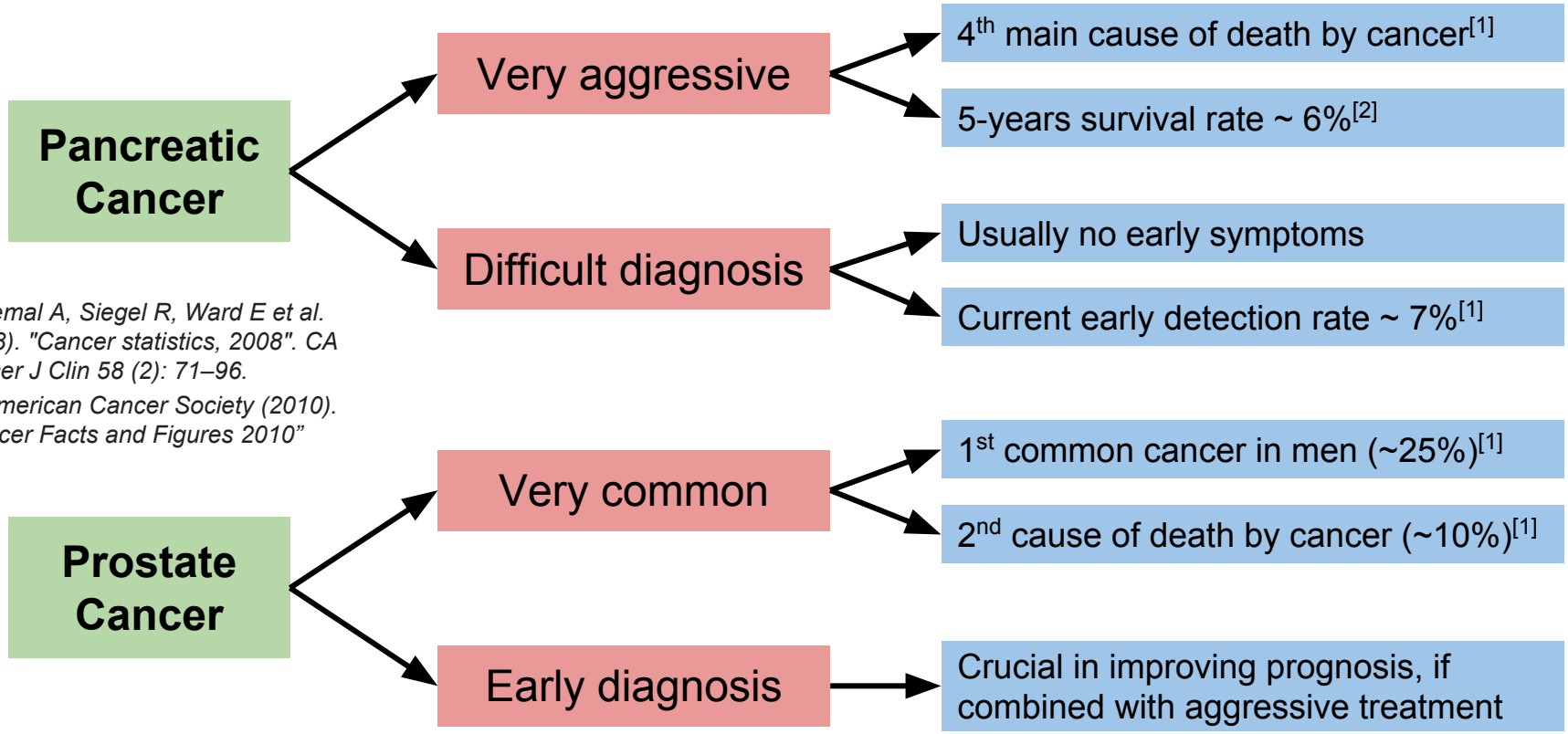

[1] Jemal A, Siegel R, Ward E et al. (2008). "Cancer statistics, 2008". CA Cancer J Clin 58 (2): 71–96.

[2] American Cancer Society (2010). "Cancer Facts and Figures 2010"

➔ Standard imaging nowadays performed with **US**, **CT** and **MRI,** not **PET**

➔ Limited effectiveness of standard **WB-PET/CT** scanners

- small organ dimensions
- background from organs nearby
- 18F-FDG not very specific

Pancreas and prostate cancers

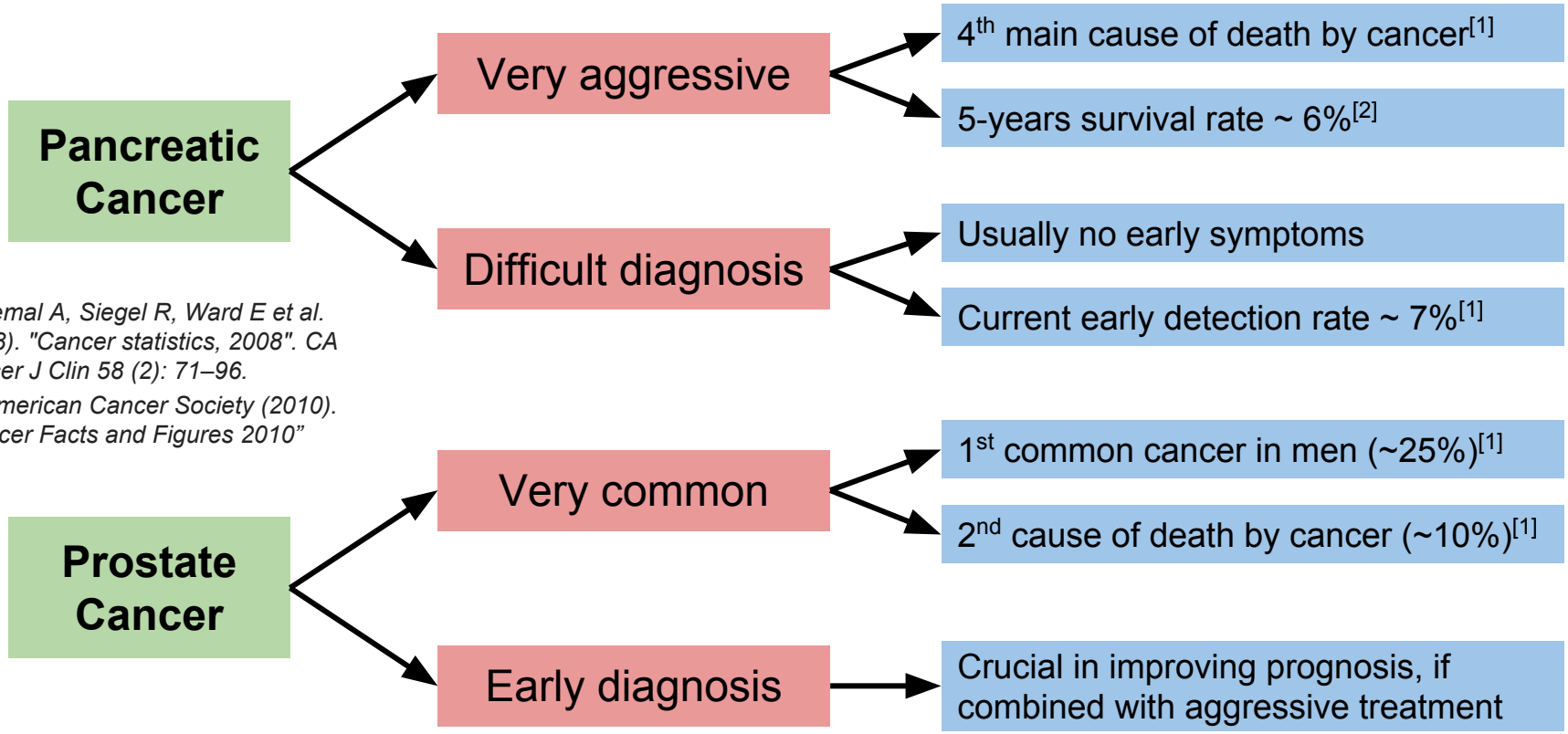

[1] Jemal A, Siegel R, Ward E et al. (2008). "Cancer statistics, 2008". CA Cancer J Clin 58 (2): 71–96.

[2] American Cancer Society (2010). "Cancer Facts and Figures 2010"

➔ Standard imaging nowadays performed with **US**, **CT** and **MRI,** not **PET**

➔ Limited effectiveness of standard **WB-PET/CT** scanners

- small organ dimensions → **High spatial resolution** **[1-2 mm]**
- background from organs nearby
- 18F-FDG not very specific

Pancreas and prostate cancers

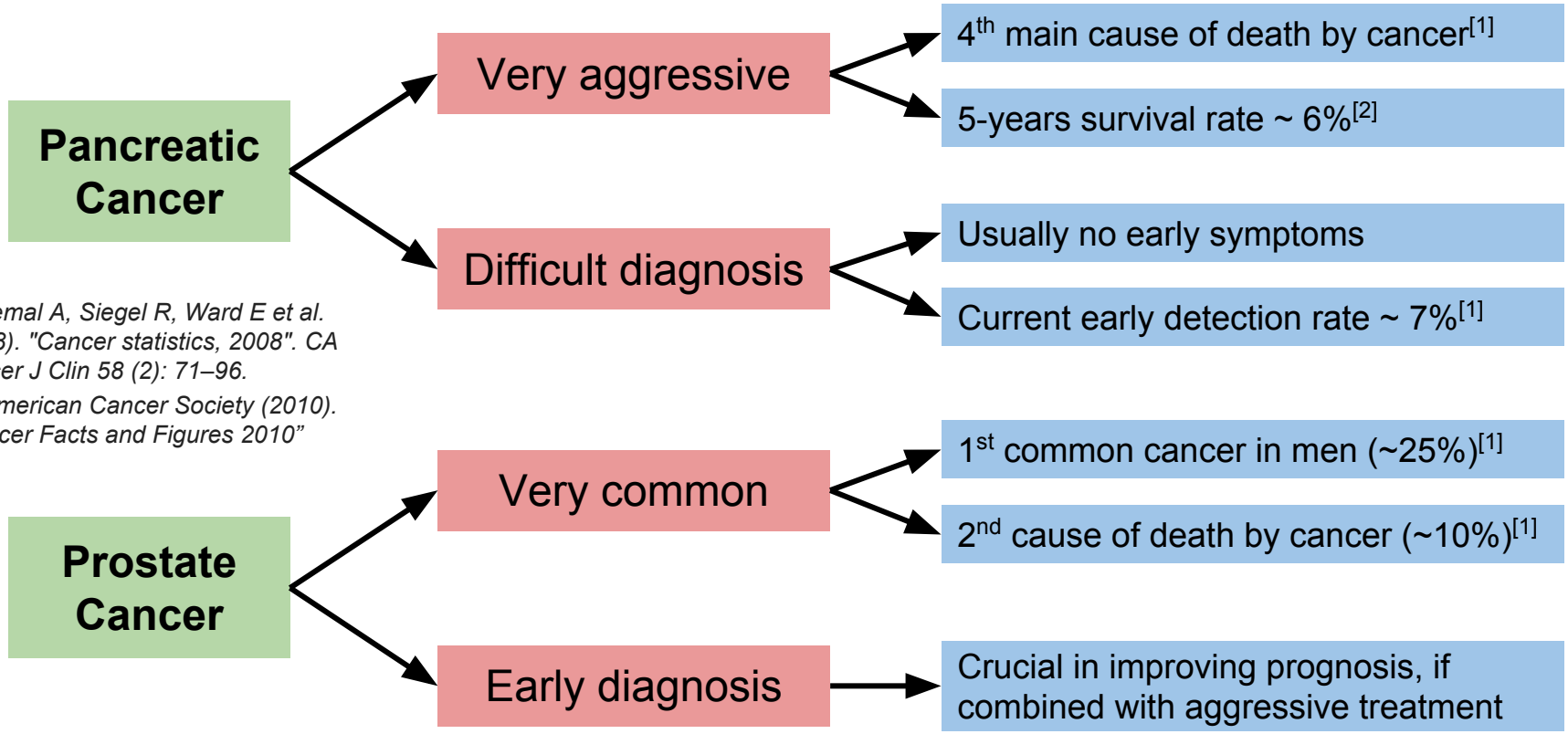

[1] Jemal A, Siegel R, Ward E et al. (2008). "Cancer statistics, 2008". CA Cancer J Clin 58 (2): 71–96.

[2] American Cancer Society (2010). "Cancer Facts and Figures 2010"

➔ Standard imaging nowadays performed with **US**, **CT** and **MRI,** not **PET**

➔ Limited effectiveness of standard **WB-PET/CT** scanners

- ➢ small organ dimensions → **High spatial resolution** **[1-2 mm]**
- ➢ background from organs nearby → **Background rejection with TOF** **[200 ps]**
- ➢ 18F-FDG not very specific

Pancreas and prostate cancers

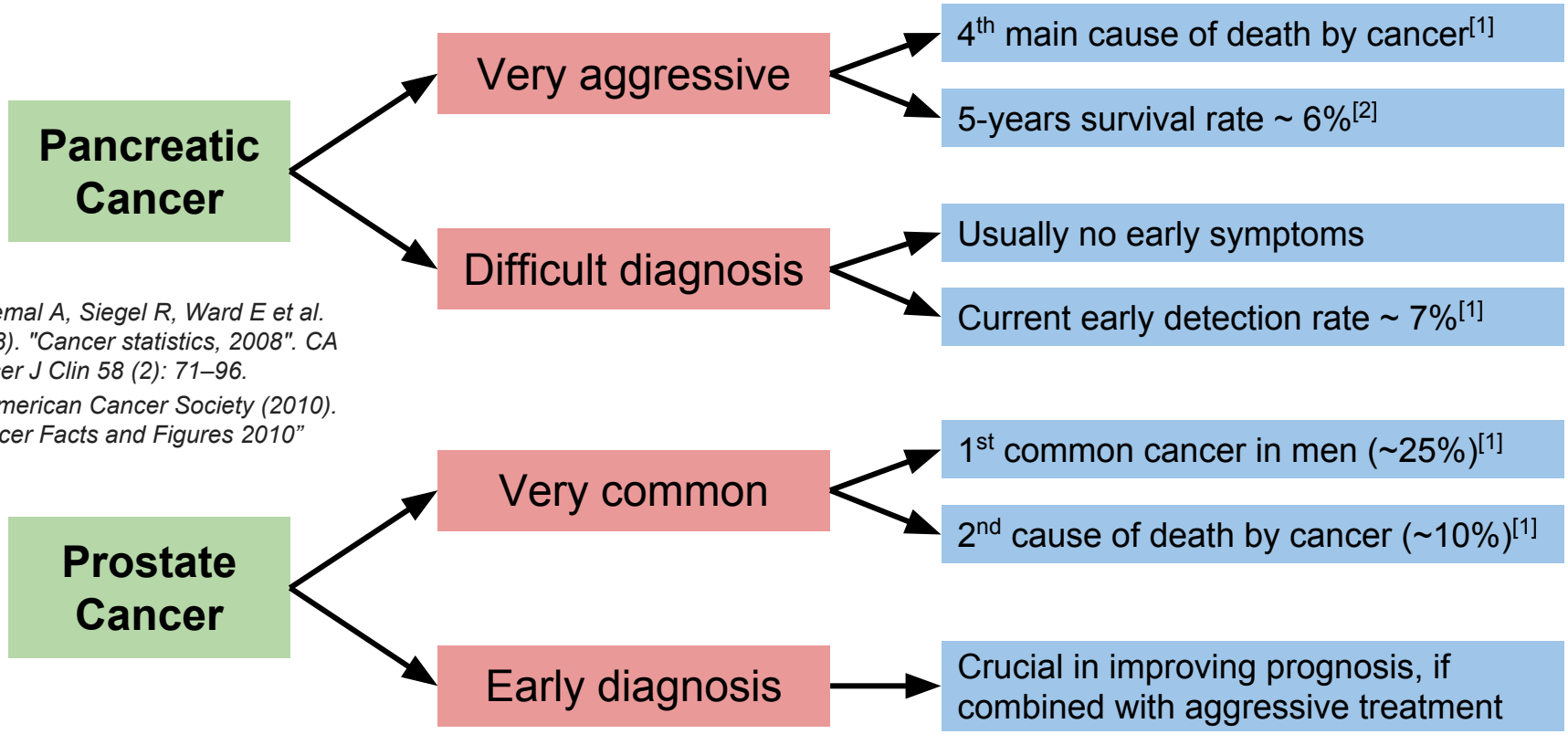

[1] Jemal A, Siegel R, Ward E et al. (2008). "Cancer statistics, 2008". CA Cancer J Clin 58 (2): 71–96.

[2] American Cancer Society (2010). "Cancer Facts and Figures 2010"

➔ Standard imaging nowadays performed with **US**, **CT** and **MRI,** not **PET**

➔ Limited effectiveness of standard **WB-PET/CT** scanners

- small organ dimensions → **High spatial resolution** **[1-2 mm]**
- background from organs nearby → **Background rejection with TOF** **[200 ps]**
- 18F-FDG not very specific → **New radiotracers**

Technological goals and challenges

Spatial resolution

$$\Delta x_{FWHM} \sim a\sqrt{\left(\frac{d}{2}\right)^2 + (0.0022D)^2 + r^2 + b^2}$$

W.W. Moses, S.E. Derenzo, J. Nucl. Med. 34 (1993) 101P

Spatial resolution

$$\Delta x_{FWHM} \sim a\sqrt{\left(\frac{d}{2}\right)^2 + (0.0022D)^2 + r^2 + b^2}$$

W.W. Moses, S.E. Derenzo, J. Nucl. Med. 34 (1993) 101P

➔ EndoTOFPET-US project goal: Δx_{FWHM} **= 1-2 mm**

Spatial resolution

$$\Delta x_{FWHM} \sim a\sqrt{\left(\frac{d}{2}\right)^2 + (0.0022D)^2 + r^2 + b^2}$$

W.W. Moses, S.E. Derenzo, J. Nucl. Med. 34 (1993) 101P

➔ EndoTOFPET-US project goal: Δx_{FWHM} **= 1-2 mm**

- ➢ **a** = reconstruction degradation **~1.25**
- ➢ **r** = positron range **~0.8 mm**

Spatial resolution

$$\Delta x_{FWHM} \sim a\sqrt{\left(\frac{d}{2}\right)^2 + (0.0022D)^2 + r^2 + b^2}$$

W.W. Moses, S.E. Derenzo, J. Nucl. Med. 34 (1993) 101P

➔ EndoTOFPET-US project goal: Δx_{FWHM} **= 1-2 mm**

- ➢ **a** = reconstruction degradation **~1.25**
- ➢ **r** = positron range **~0.8 mm**
- ➢ **d** = crystal transversal size **0.75 mm**
- ➢ **D** = detector heads distance **< 100 mm**
- ➢ **b** = accuracy of positioning system **< 1 mm**

Spatial resolution

$$\Delta x_{FWHM} \sim a\sqrt{\left(\frac{d}{2}\right)^2 + (0.0022D)^2 + r^2 + b^2}$$

W.W. Moses, S.E. Derenzo, J. Nucl. Med. 34 (1993) 101P

➔ EndoTOFPET-US project goal: Δx_{FWHM} **= 1-2 mm**

- ➢ **a** = reconstruction degradation **~1.25**
- ➢ **r** = positron range **~0.8 mm**
- ➢ **d** = crystal transversal size **0.75 mm**
- ➢ **D** = detector heads distance **< 100 mm**
- ➢ **b** = accuracy of positioning system **< 1 mm**

➔ High **granularity**

➔ **Endoscopic** approach

Background rejection

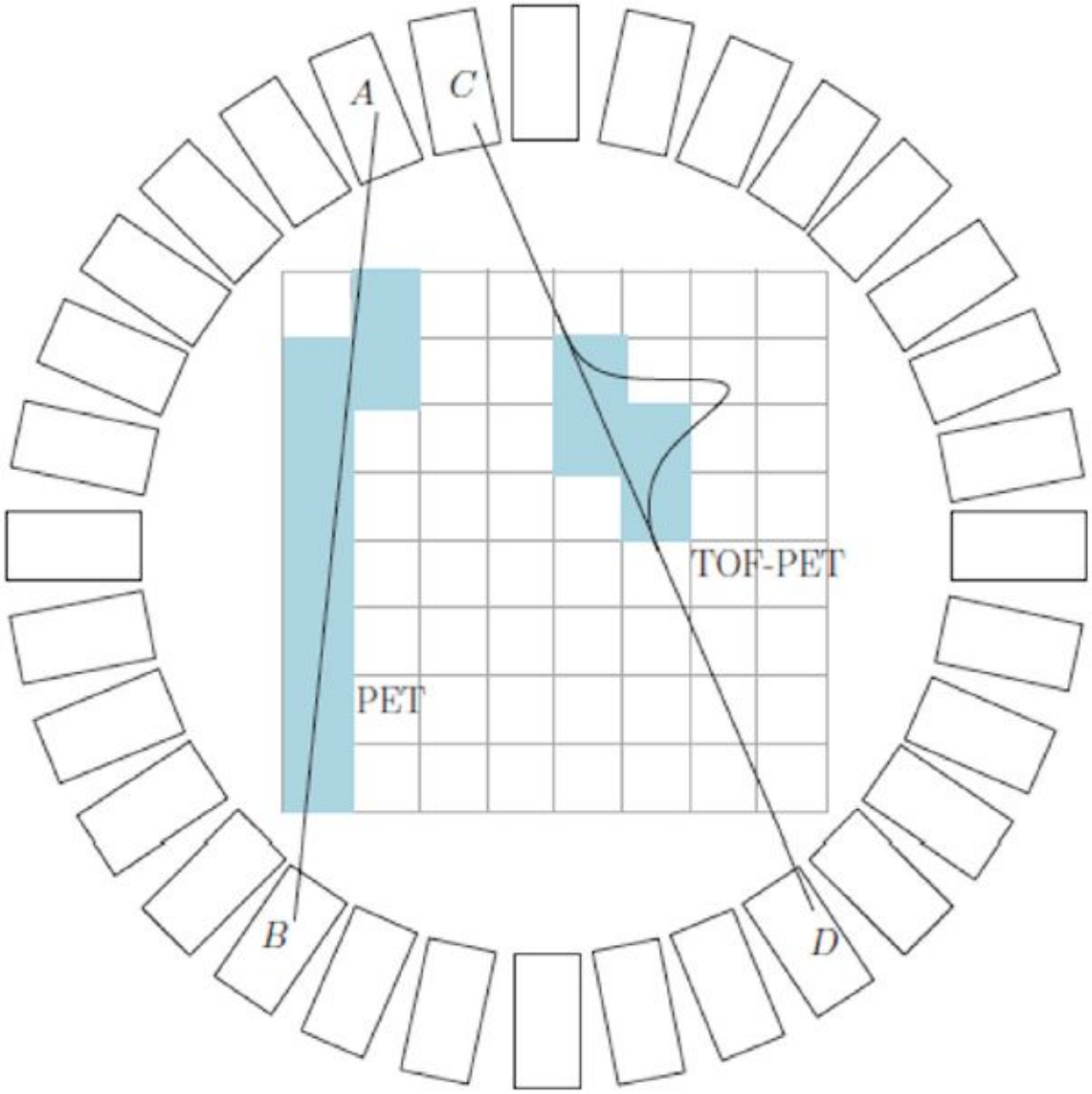

S. Surti, J.S. Karp - Physica Medica 32 (2016) 12–22

Time of Flight (TOF)

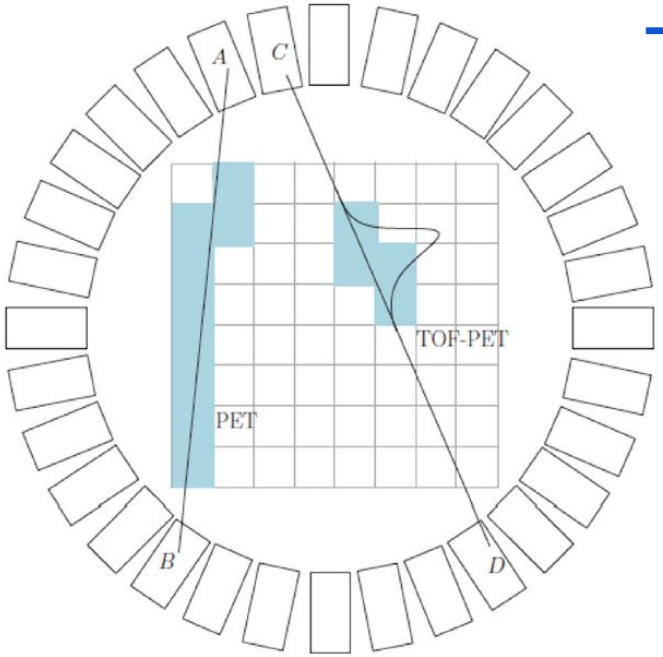

S. Surti, J.S. Karp - Physica Medica 32 (2016) 12–22

➔ Compute the **difference in time of arrival** of gammas:

Time of Flight (TOF)

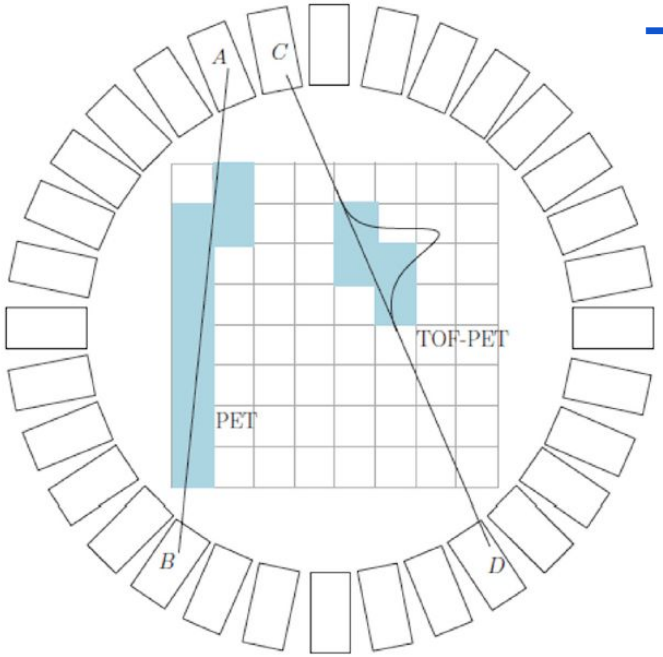

S. Surti, J.S. Karp - Physica Medica 32 (2016) 12–22

➔ Compute the **difference in time of arrival** of gammas:

➢ Improve event localization along LORs, reject events from nearby organs (liver, heart, bladder)

$$\Delta x = c\frac{\Delta t}{2}$$

Time of Flight (TOF)

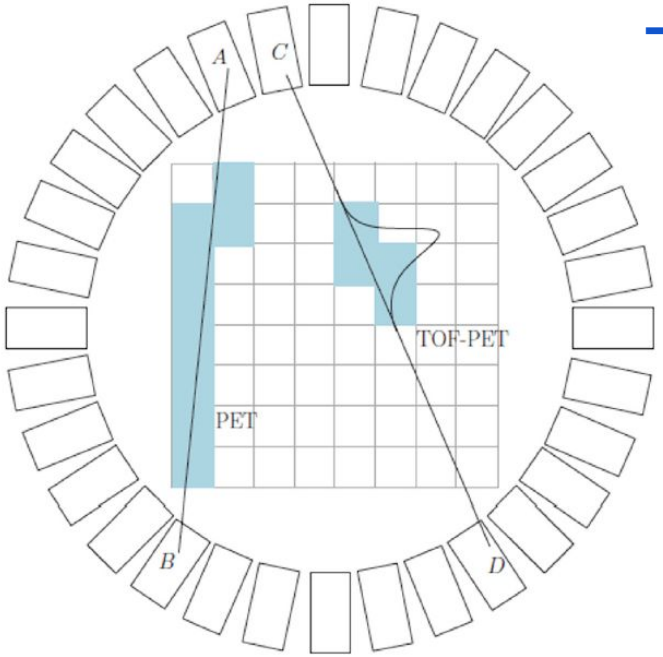

S. Surti, J.S. Karp - Physica Medica 32 (2016) 12–22

➔ Compute the **difference in time of arrival** of gammas:

- Improve event localization along LORs, reject events from nearby organs (liver, heart, bladder)

$$\Delta x = c\frac{\Delta t}{2}$$

- Decrease noise correlation in overlapping LORs, improve Signal-to-Noise Ratio (SNR)

$$SNR_{TOF} \sim \sqrt{\frac{D}{\Delta x}} \cdot SNR_{CONV}$$

D = effective object diameter

Time of Flight (TOF)

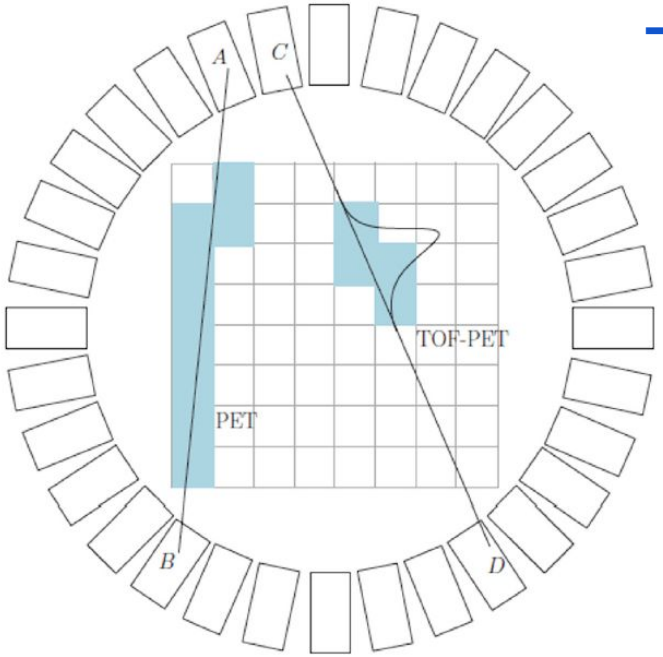

S. Surti, J.S. Karp - Physica Medica 32 (2016) 12–22

➔ Compute the **difference in time of arrival** of gammas:

- ➢ Improve event localization along LORs, reject events from nearby organs (liver, heart, bladder)

$$\Delta x = c\frac{\Delta t}{2}$$

- ➢ Decrease noise correlation in overlapping LORs, improve Signal-to-Noise Ratio (SNR)

$$SNR_{TOF} \sim \sqrt{\frac{D}{\Delta x}} \cdot SNR_{CONV}$$

D = effective object diameter

Time resolution (ns)	Δx (cm)	TOF NEC gain	TOF SNR gain
0.1	1.5	26.7	5.2
0.3	4.5	8.9	3.0
0.6	9.0	4.4	2.1
1.2	18.0	2.2	1.5
2.7	40.0	1.0	1.0

M. Conti - Eur J Nucl Med Mol Imaging (2011) 38:1147–1157

Time of Flight (TOF)

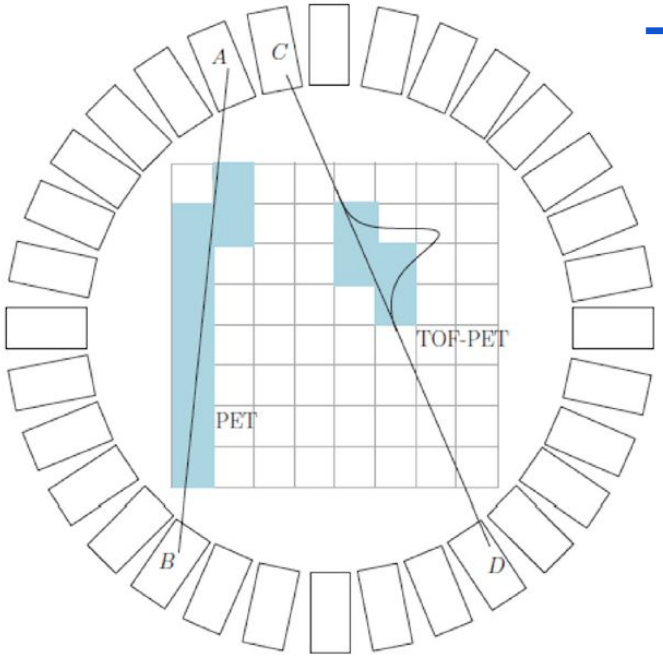

S. Surti, J.S. Karp - Physica Medica 32 (2016) 12–22

➔ Compute the **difference in time of arrival** of gammas:

- ➢ Improve event localization along LORs, reject events from nearby organs (liver, heart, bladder)

$$\Delta x = c\frac{\Delta t}{2}$$

- ➢ Decrease noise correlation in overlapping LORs, improve Signal-to-Noise Ratio (SNR)

$$SNR_{TOF} \sim \sqrt{\frac{D}{\Delta x}} \cdot SNR_{CONV}$$

D = effective object diameter

Time resolution (ns)	Δx (cm)	TOF NEC gain	TOF SNR gain
0.1	1.5	26.7	5.2
0.3	4.5	8.9	3.0
0.6	9.0	4.4	2.1
1.2	18.0	2.2	1.5
2.7	40.0	1.0	1.0

M. Conti - Eur J Nucl Med Mol Imaging (2011) 38:1147–1157

➔ Current commercial PET scanner

- ➢ **Δt_{FWHM} = 450 ps (250 ps)**

Time of Flight (TOF)

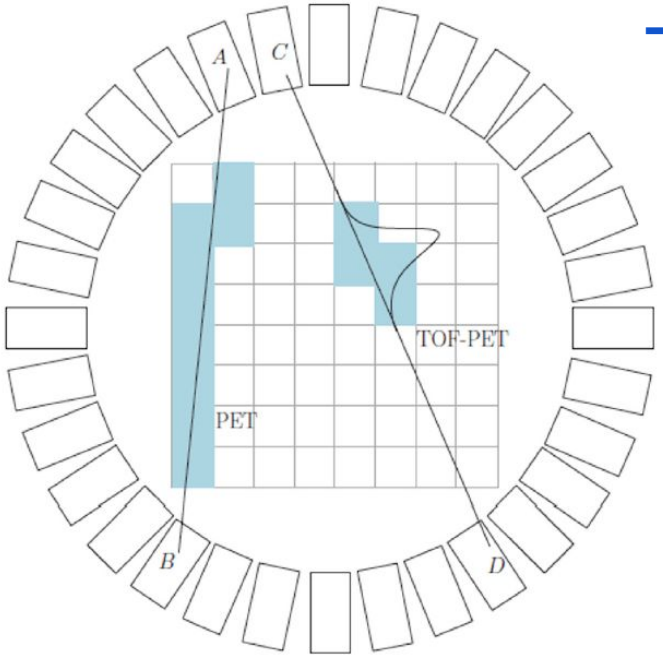

S. Surti, J.S. Karp - Physica Medica 32 (2016) 12–22

➔ Compute the **difference in time of arrival** of gammas:

- ➢ Improve event localization along LORs, reject events from nearby organs (liver, heart, bladder)

$$\Delta x = c\frac{\Delta t}{2}$$

- ➢ Decrease noise correlation in overlapping LORs, improve Signal-to-Noise Ratio (SNR)

$$SNR_{TOF} \sim \sqrt{\frac{D}{\Delta x}} \cdot SNR_{CONV}$$

D = effective object diameter

Time resolution (ns)	Δx (cm)	TOF NEC gain	TOF SNR gain
0.1	1.5	26.7	5.2
0.3	4.5	8.9	3.0
0.6	9.0	4.4	2.1
1.2	18.0	2.2	1.5
2.7	40.0	1.0	1.0

M. Conti - Eur J Nucl Med Mol Imaging (2011) 38:1147–1157

➔ Current commercial PET scanner

- ➢ **Δt_{FWHM} = 450 ps (250 ps)**

➔ Project goal

- ➢ **Δt_{FWHM} = 200 ps → x = 3cm**

Benefits of TOF

➔ Improved **lesion detectability** while keeping scanning time constant

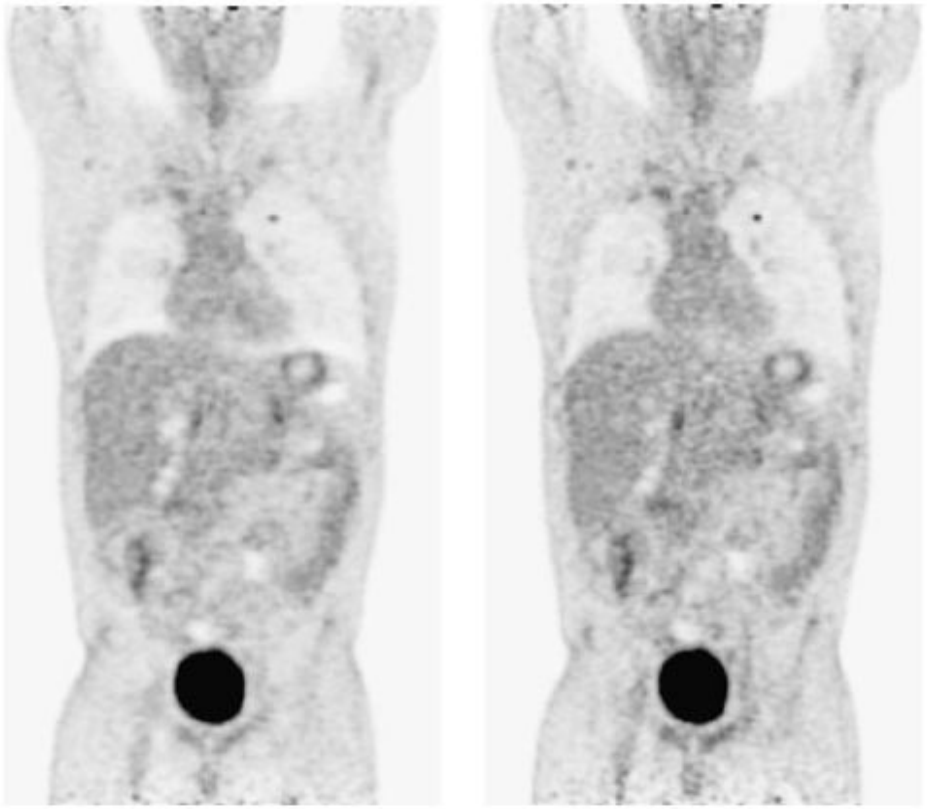

Fig. 1 Coronal images reconstructed from a non-TOF scan (*left*) and a TOF scan (*right*) in a patient with lung cancer. The acquisition time was 3 min per bed position for both images. At the same number of counts, the image quality is better with the TOF reconstruction

M. Conti - Eur J Nucl Med Mol Imaging (2011) 38:1147–1157

Benefits of TOF

➔ Improved **lesion detectability** while keeping scanning time constant

➔ Reduced **scan times** for the same lesion detectability

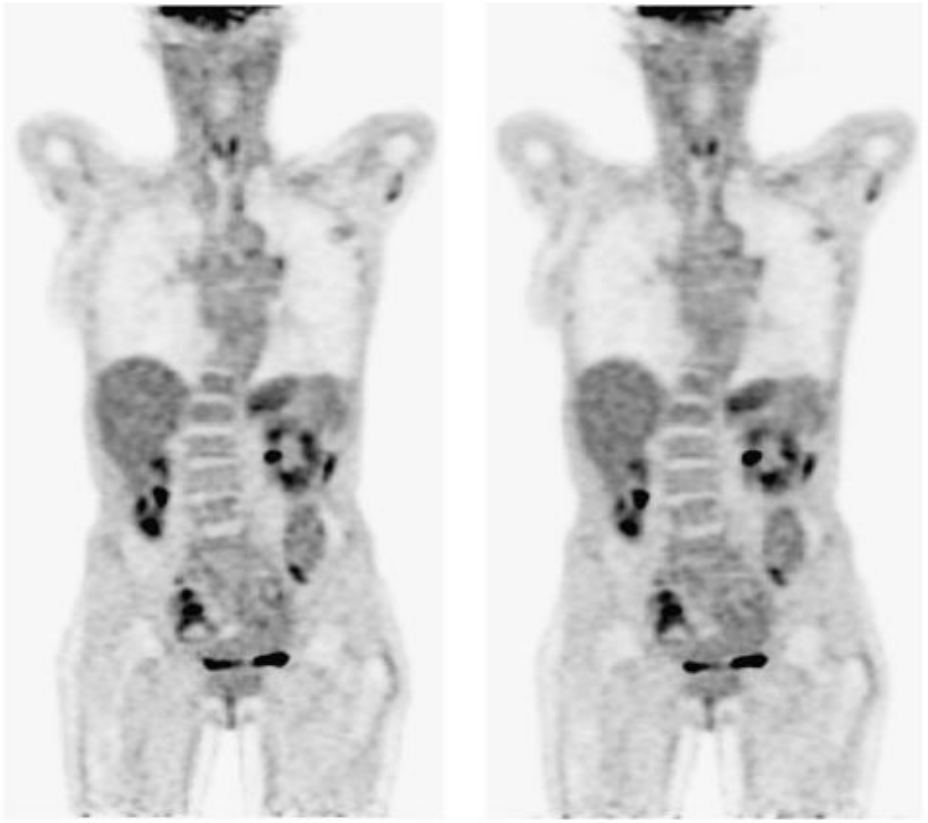

Fig. 2 Coronal images reconstructed from a non-TOF scan (*left*) and a TOF scan (*right*). The acquisition time was 2 min per bed position for the non-TOF scan and 1 min per bed position for the TOF scan. The quality of the non-TOF image and that of the TOF image with half of the counts are similar

M. Conti - Eur J Nucl Med Mol Imaging (2011) 38:1147–1157

Benefits of TOF

➔ Improved **lesion detectability** while keeping scanning time constant

➔ Reduced **scan times** for the same lesion detectability

➔ **Fewer iterations** of reconstruction algorithms required to maximize lesion contrast -> lower image noise

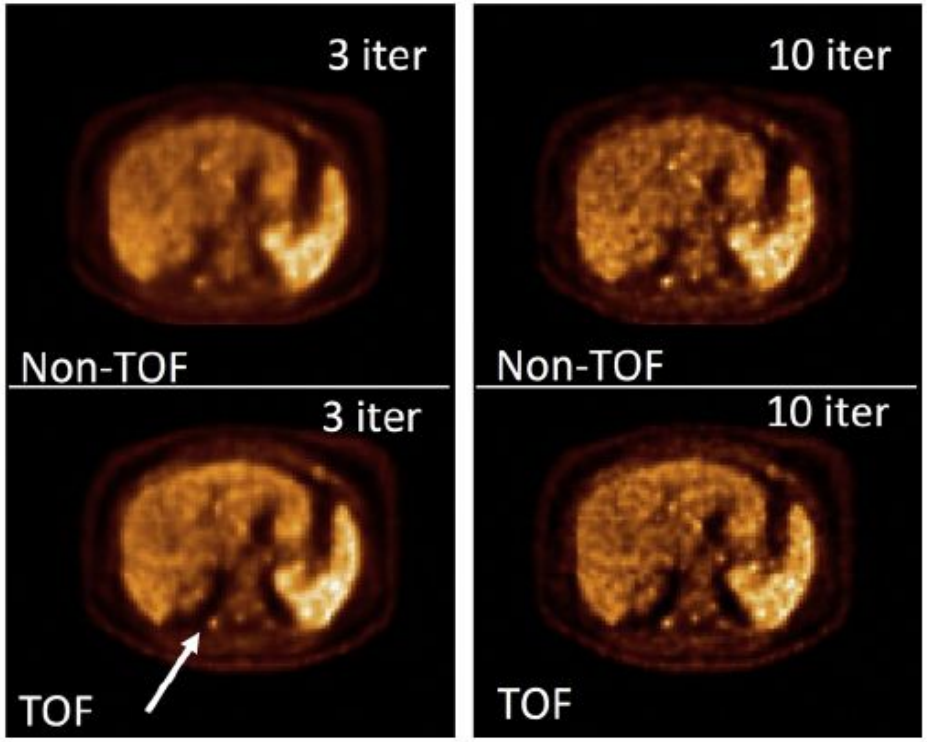

Figure 2. Reconstructed transverse slices of a clinical ^{18}F-FDG study. As indicated, images are shown for Non-TOF and TOF reconstruction and for iterations 3 and 10 of the reconstruction algorithm. The arrow indicates the lesion for which an accurate SUV is measured after 3 iterations of the TOF reconstruction algorithm.

S. Surti, J.S. Karp - Physica Medica 32 (2016) 12–22

Benefits of TOF

- ➔ Improved **lesion detectability** while keeping scanning time constant
- ➔ Reduced **scan times** for the same lesion detectability
- ➔ **Fewer iterations** of reconstruction algorithms required to maximize lesion contrast -> lower image noise
- ➔ Better lesion detectability for **larger objects**

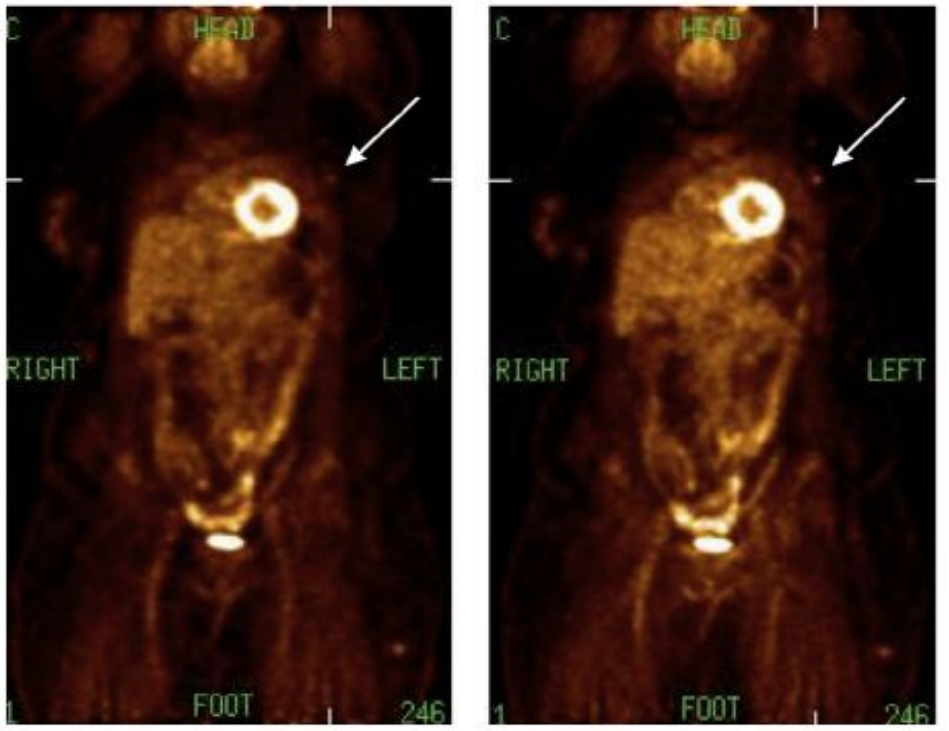

Reconstructed coronal slices of an 18F-FDG study for a heavy (140 kg) patient diagnosed with non-Hodgkins lymphoma. The images are (left) Non-TOF reconstruction and (right) TOF reconstruction using all collected counts. Arrows indicate a lesion that has higher uptake and is better discriminated in the TOF image.

S. Surti, J.S. Karp - Physica Medica 32 (2016) 12–22

Benefits of TOF

➔ Improved **lesion detectability** while keeping scanning time constant

➔ Reduced **scan times** for the same lesion detectability

➔ **Fewer iterations** of reconstruction algorithms required to maximize lesion contrast -> lower image noise

➔ Better lesion detectability for **larger objects**

➔ Better image reconstruction for **limited angle** PET acquisitions

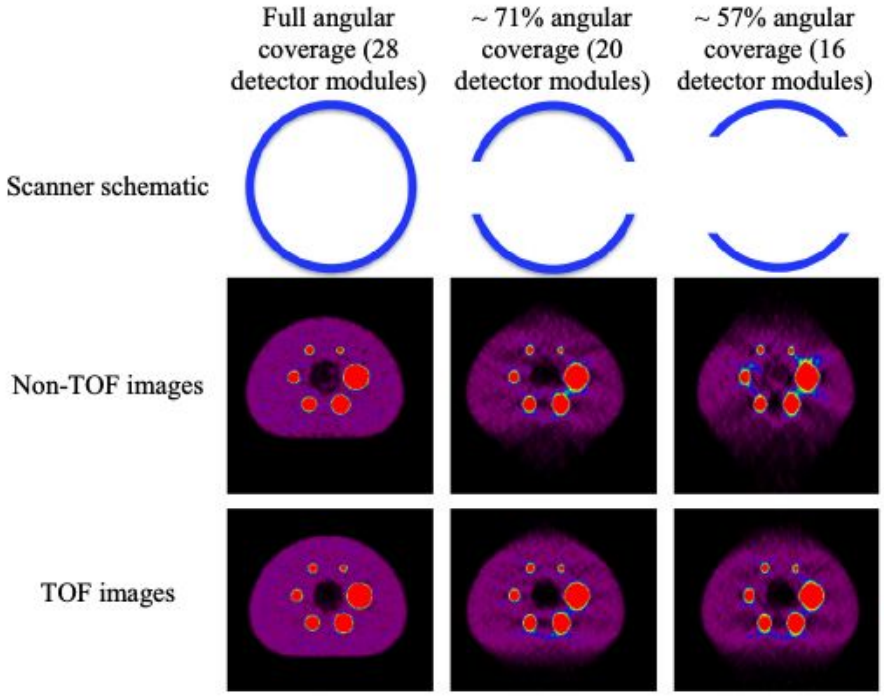

Figure 4. Reconstructed images from a NEMA image quality phantom using full or partial angular data acquired on a clinical TOF PET/CT. The six hot spheres in a ring have diameters of 37, 28, 22, 17, 13, and 10 mm and have an activity uptake of 9.7:1 with respect to background. The central cold region is a lung insert.

S. Surti, J.S. Karp - Physica Medica 32 (2016) 12–22

EndoTOFPET and the next frontier

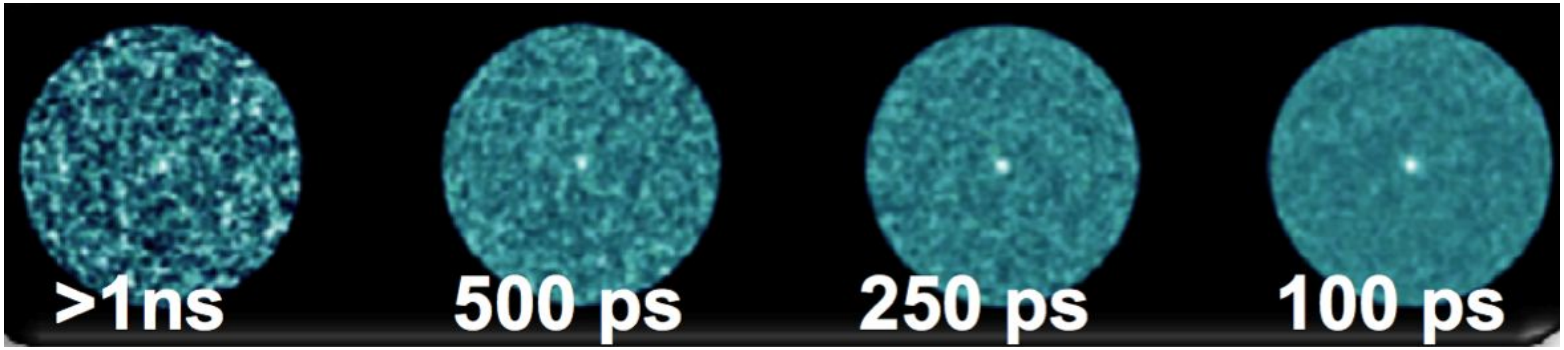

EndoTOFPET and the next frontier

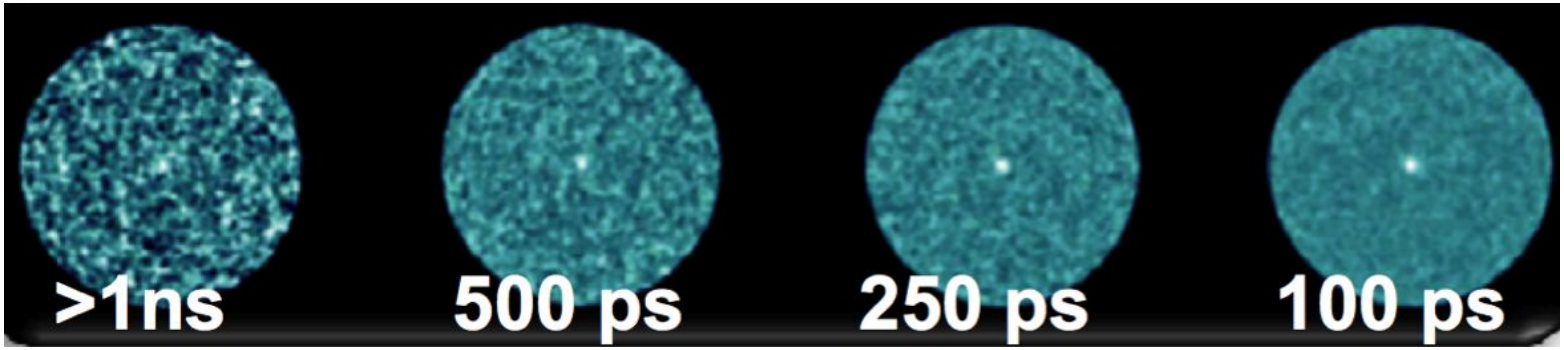

➔ **@200ps CTR** → Background rejection

EndoTOFPET and the next frontier

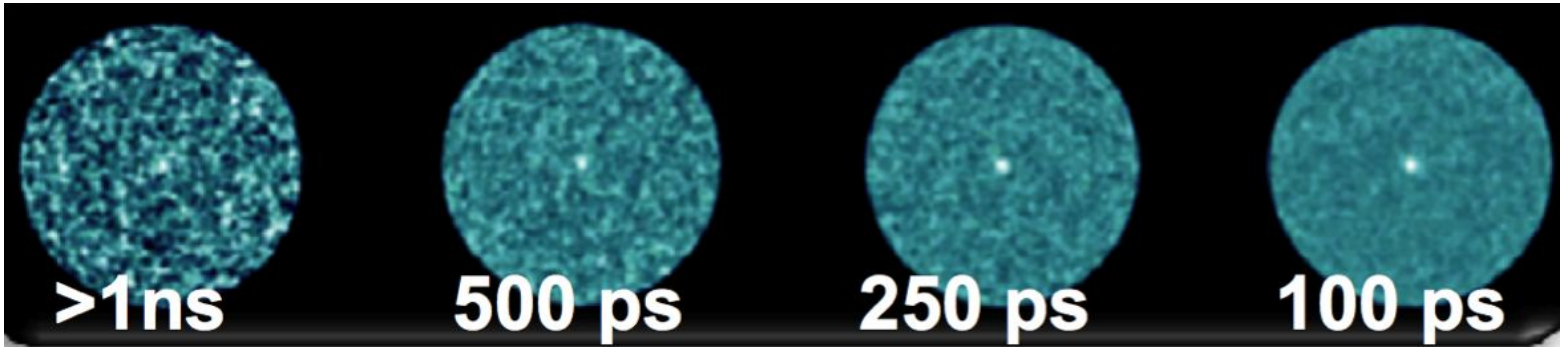

- ➔ **@200ps CTR** → Background rejection
- ➔ **@100ps CTR** → SNR improved by factor 5

EndoTOFPET and the next frontier

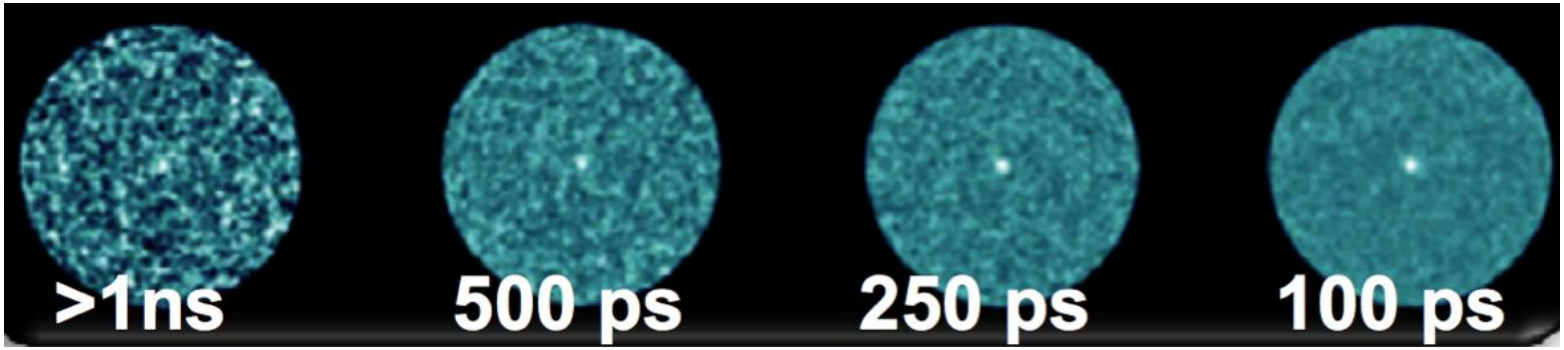

- ➔ **@200ps CTR** → Background rejection
- ➔ **@100ps CTR** → SNR improved by factor 5
- ➔ **@ 10ps CTR** → Access to **direct 3D information**

Road to 10 ps

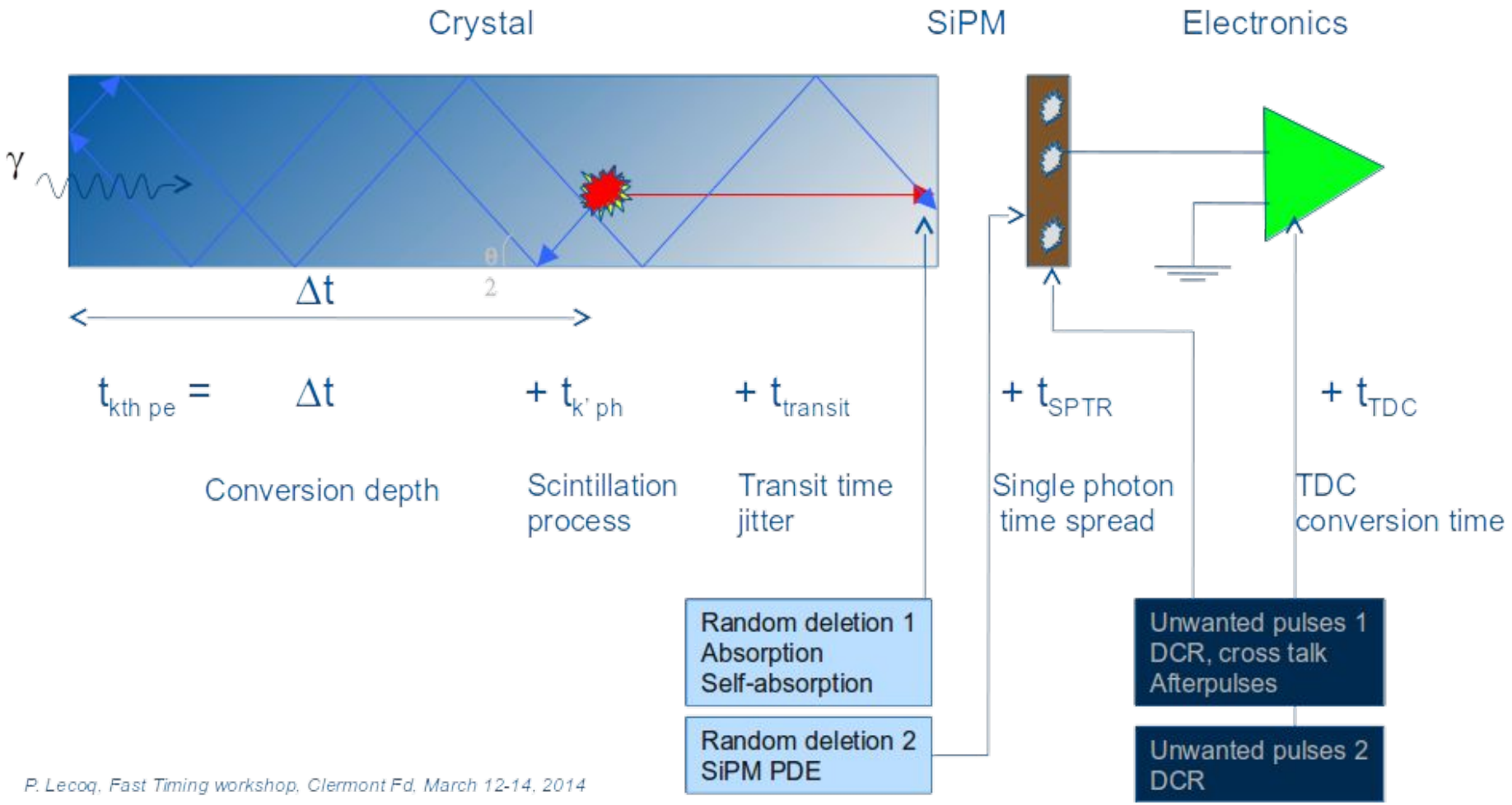

P. Lecoq, Fast Timing workshop, Clermont Fd, March 12-14, 2014

Detector design

PET detector design: external plate

➔ **Two plates** produced (one for prostate detector, one for pancreas detector)

PET detector design: external plate

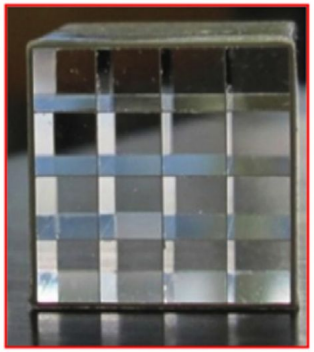

- ➔ **Two plates** produced (one for prostate detector, one for pancreas detector)
- ➔ 256 arrays of 4x4 **LYSO:Ce** scintillators for each plate
  - ➢ Individual crystal size: **3.5x3.5x15 mm^2** for prostate, **3.1x3.1x15 mm^2** for pancreas
  - ➢ Crystal pitch: **3.6 mm** for prostate, **3.2 mm** for pancreas
  - ➢ Coating material: **ESR** by 3M

PET detector design: external plate

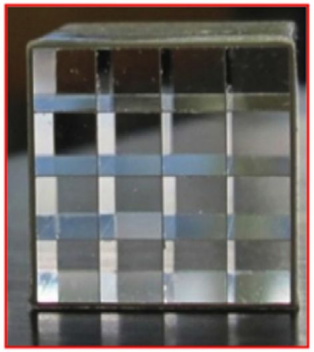

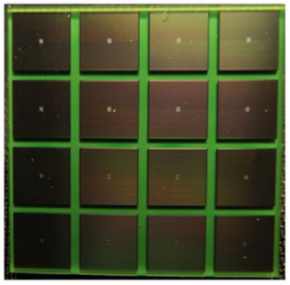

- ➔ **Two plates** produced (one for prostate detector, one for pancreas detector)
- ➔ 256 arrays of 4x4 **LYSO:Ce** scintillators for each plate
  - ➢ Individual crystal size: **3.5x3.5x15 mm^2** for prostate, **3.1x3.1x15 mm^2** for pancreas
  - ➢ Crystal pitch: **3.6 mm** for prostate, **3.2 mm** for pancreas
  - ➢ Coating material: **ESR** by 3M
- ➔ Discrete Silicon-through-via (TSV) **MPPCs** by Hamamatsu, RTV 3145 glue

PET detector design: external plate

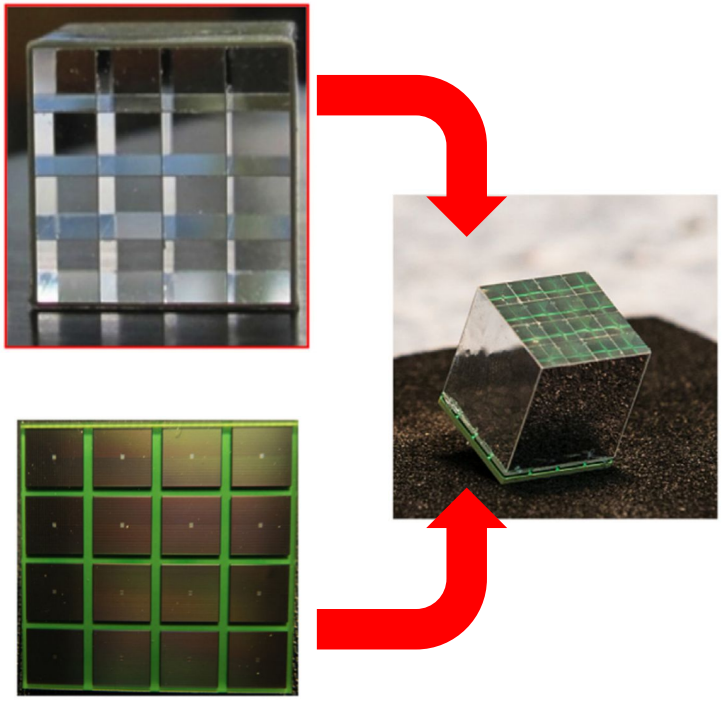

- **Two plates** produced (one for prostate detector, one for pancreas detector)
- 256 arrays of 4x4 **LYSO:Ce** scintillators for each plate
  - Individual crystal size: **3.5x3.5x15 mm^2** for prostate, **3.1x3.1x15 mm^2** for pancreas
  - Crystal pitch: **3.6 mm** for prostate, **3.2 mm** for pancreas
  - Coating material: **ESR** by 3M
- Discrete Silicon-through-via (TSV) **MPPCs** by Hamamatsu, RTV 3145 glue

PET detector design: external plate

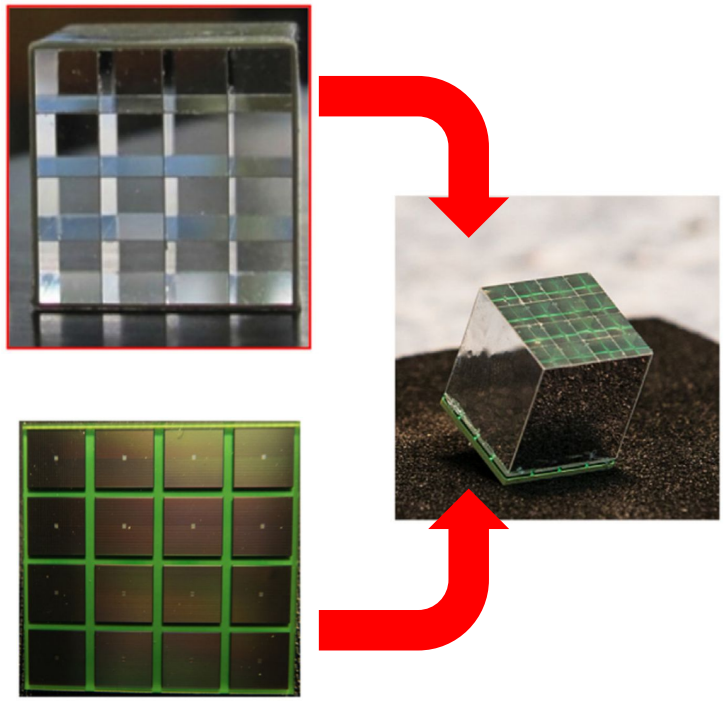

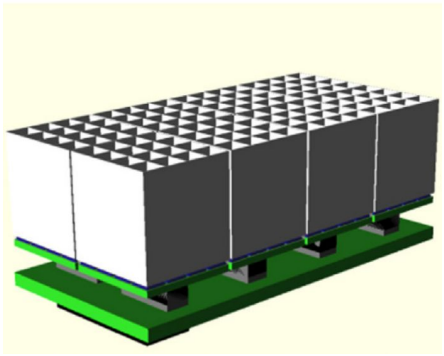

- **Two plates** produced (one for prostate detector, one for pancreas detector)
- 256 arrays of 4x4 **LYSO:Ce** scintillators for each plate
  - Individual crystal size: **3.5x3.5x15 mm^2** for prostate, **3.1x3.1x15 mm^2** for pancreas
  - Crystal pitch: **3.6 mm** for prostate, **3.2 mm** for pancreas
  - Coating material: **ESR** by 3M
- Discrete Silicon-through-via (TSV) **MPPCs** by Hamamatsu, RTV 3145 glue
- **FEB/A** with 8 modules and 2x64ch readout **ASICs**, 4 **FEB/D** with 8 FEB/A each

PET detector design: external plate

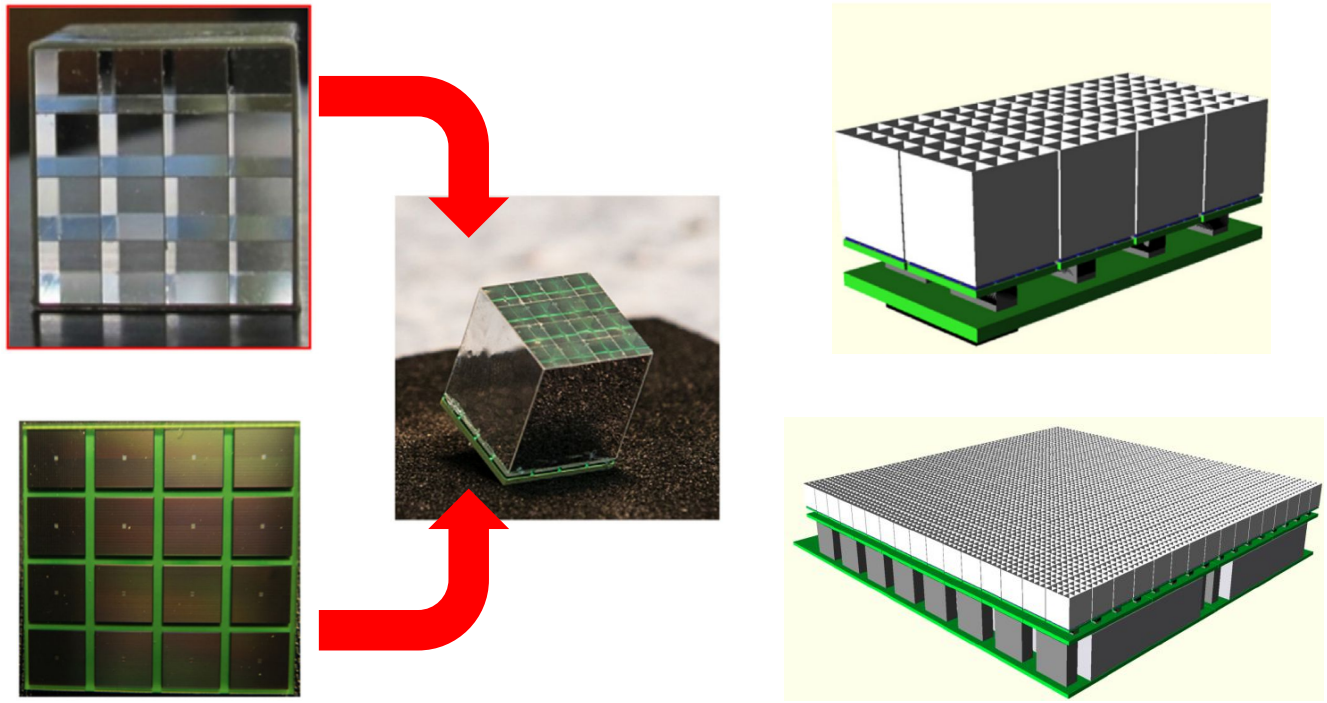

- ➔ **Two plates** produced (one for prostate detector, one for pancreas detector)
- ➔ 256 arrays of 4x4 **LYSO:Ce** scintillators for each plate
  - ➢ Individual crystal size: **3.5x3.5x15 mm^2** for prostate, **3.1x3.1x15 mm^2** for pancreas
  - ➢ Crystal pitch: **3.6 mm** for prostate, **3.2 mm** for pancreas
  - ➢ Coating material: **ESR** by 3M
- ➔ Discrete Silicon-through-via (TSV) **MPPCs** by Hamamatsu, RTV 3145 glue
- ➔ **FEB/A** with 8 modules and 2x64ch readout **ASICs**, 4 **FEB/D** with 8 FEB/A each

PET detector design: external plate

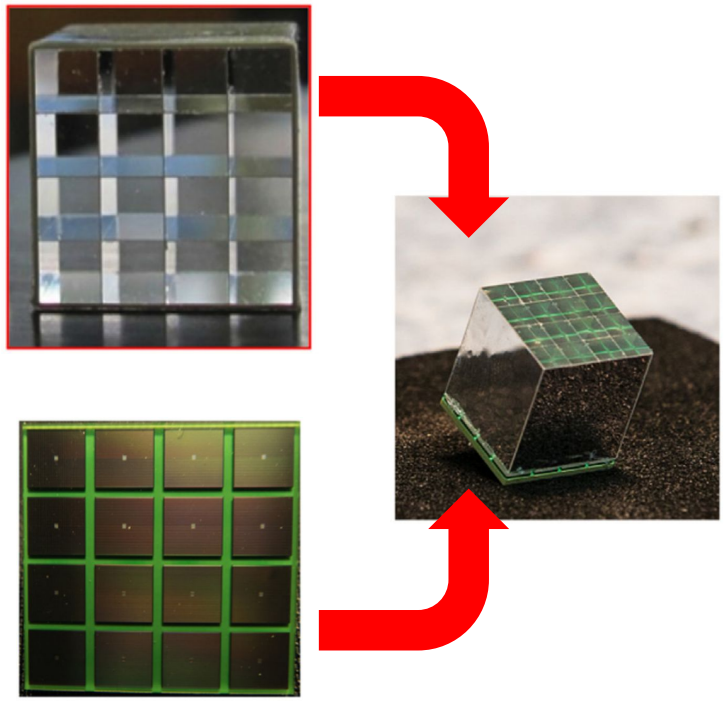

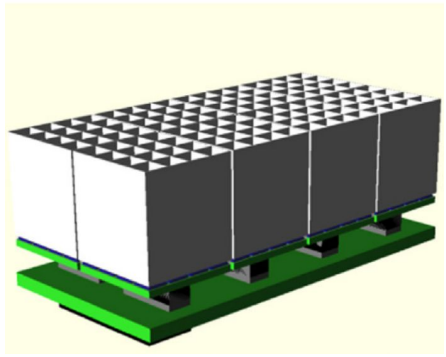

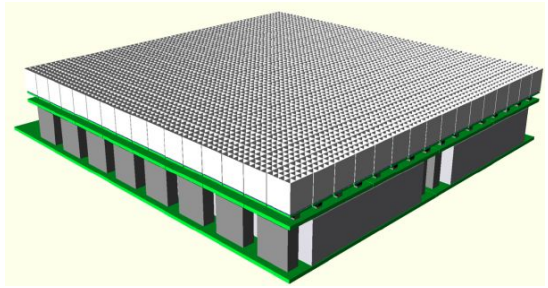

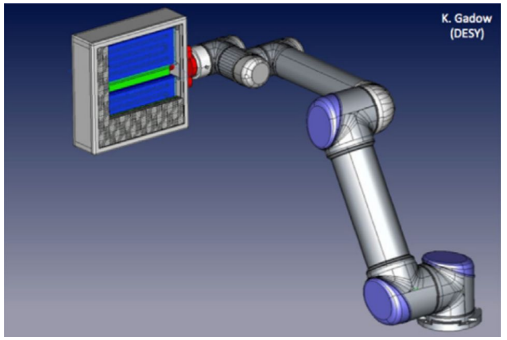

- ➔ **Two plates** produced (one for prostate detector, one for pancreas detector)
- ➔ 256 arrays of 4x4 **LYSO:Ce** scintillators for each plate
  - ➢ Individual crystal size: **3.5x3.5x15 mm^2** for prostate, **3.1x3.1x15 mm^2** for pancreas
  - ➢ Crystal pitch: **3.6 mm** for prostate, **3.2 mm** for pancreas
  - ➢ Coating material: **ESR** by 3M
- ➔ Discrete Silicon-through-via (TSV) **MPPCs** by Hamamatsu, RTV 3145 glue
- ➔ **FEB/A** with 8 modules and 2x64ch readout **ASICs**, 4 **FEB/D** with 8 FEB/A each
- ➔ Cooling system, mechanical arm

PET detector design: external plate

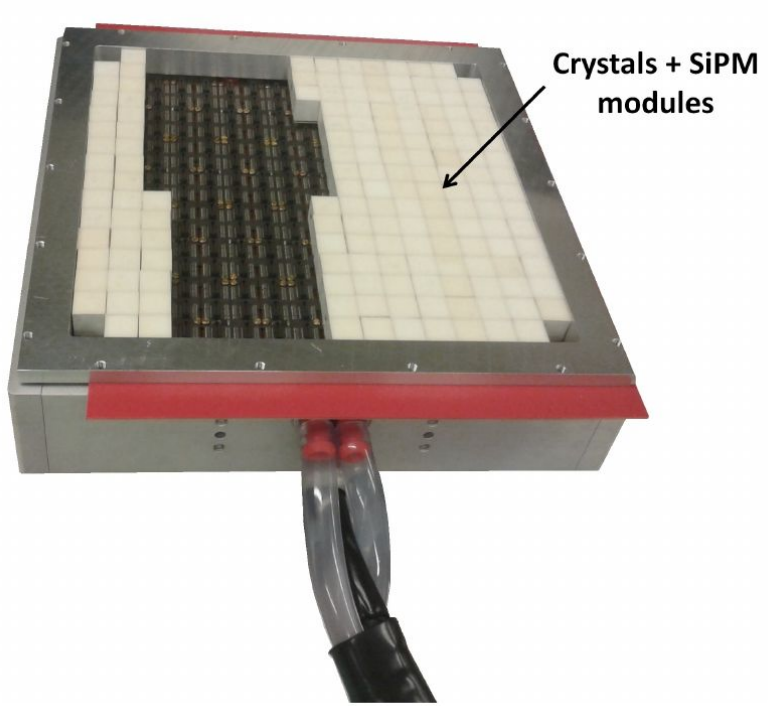

- ➔ **Two plates** produced (one for prostate detector, one for pancreas detector)
- ➔ 256 arrays of 4x4 **LYSO:Ce** scintillators for each plate
  - ➢ Individual crystal size: **3.5x3.5x15 mm^2** for prostate, **3.1x3.1x15 mm^2** for pancreas
  - ➢ Crystal pitch: **3.6 mm** for prostate, **3.2 mm** for pancreas
  - ➢ Coating material: **ESR** by 3M
- ➔ Discrete Silicon-through-via (TSV) **MPPCs** by Hamamatsu, RTV 3145 glue
- ➔ **FEB/A** with 8 modules and 2x64ch readout **ASICs**, 4 **FEB/D** with 8 FEB/A each
- ➔ Cooling system, mechanical arm

PET detector design: endoscopic probe

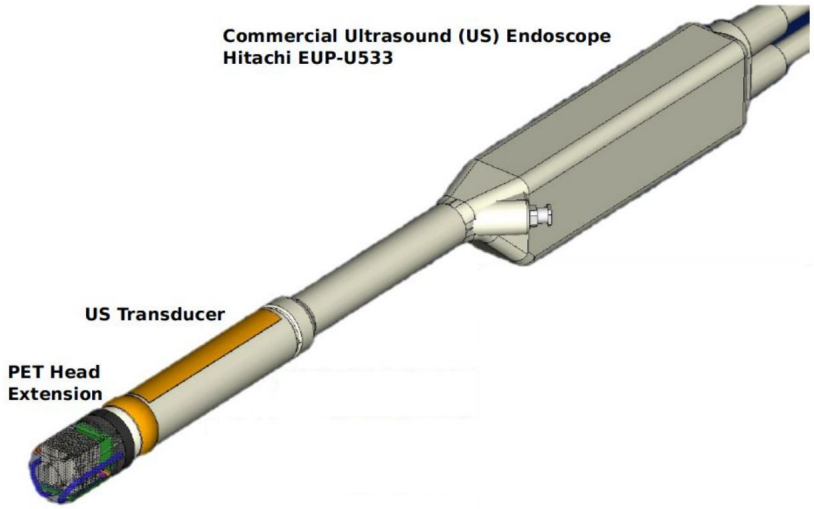

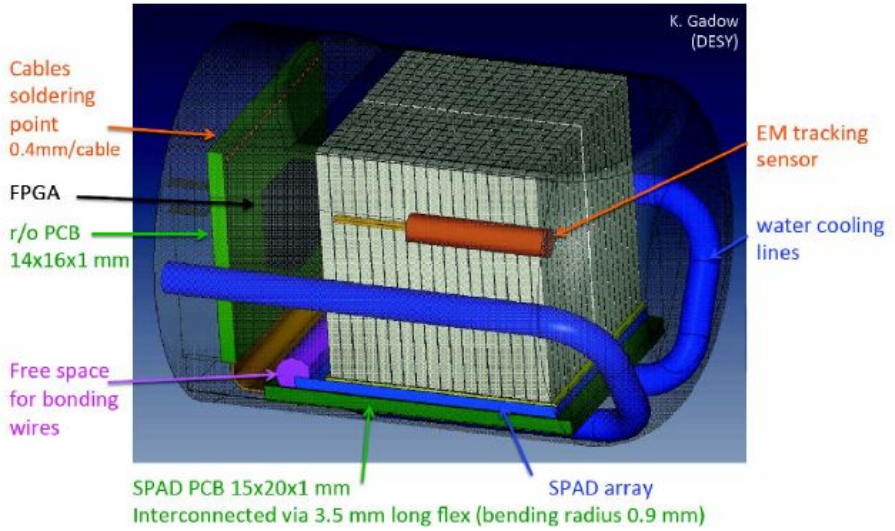

➔ **Two different versions** under development:

PET detector design: endoscopic probe

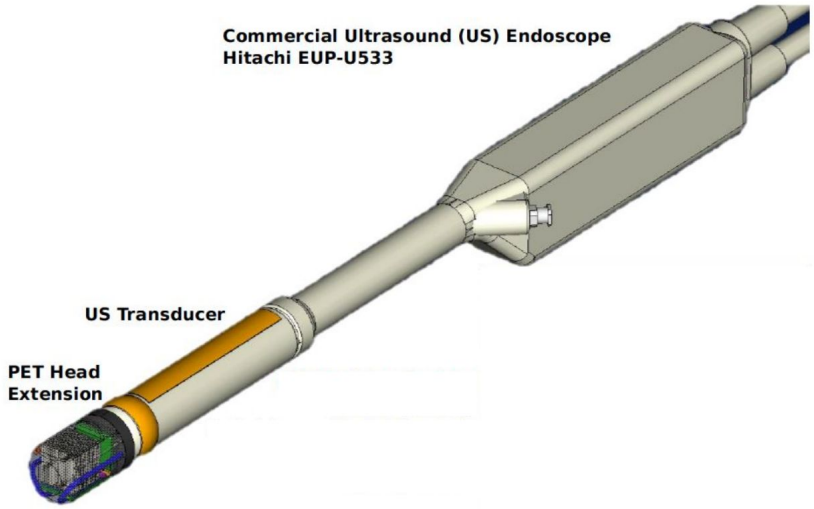

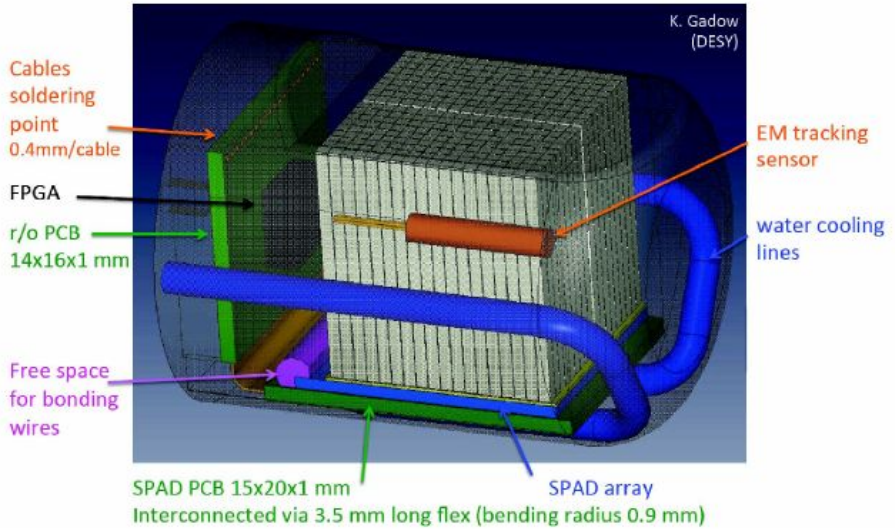

➔ **Two different versions** under development:

- ➢ Pancreas probe, diameter **15 mm**
  - Clamped on Fujinon EG-530UR2

PET detector design: endoscopic probe

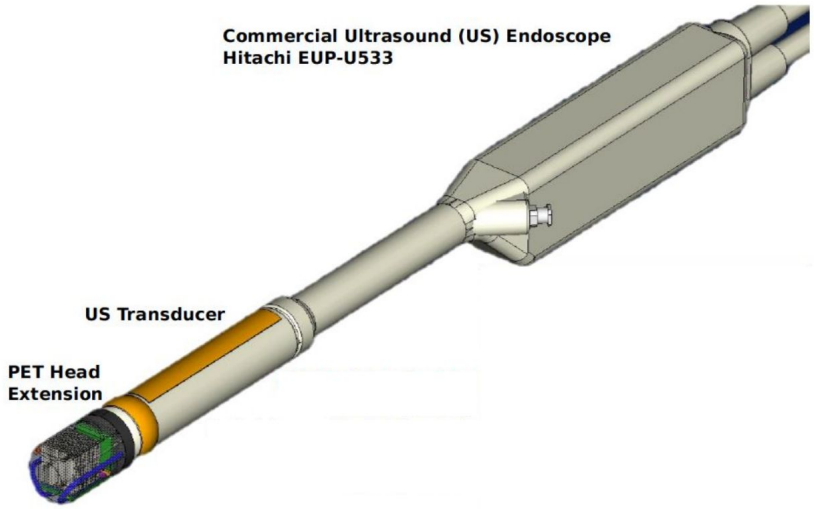

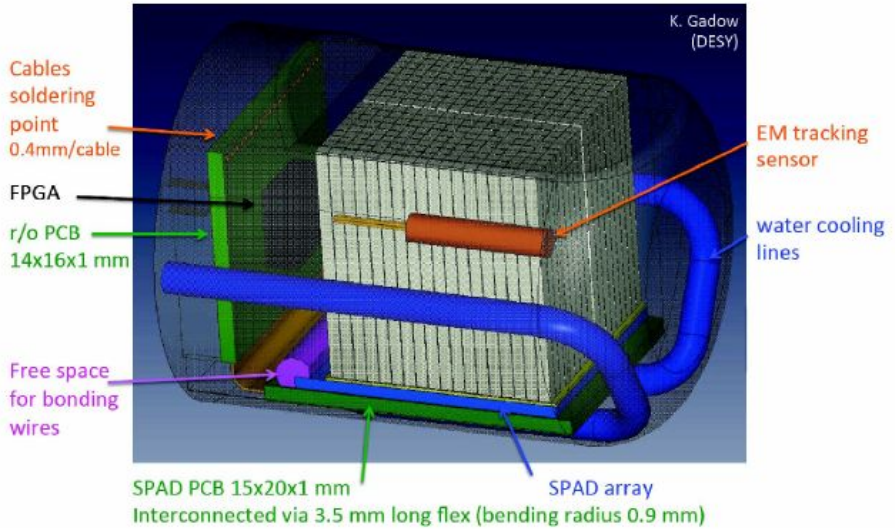

➔ **Two different versions** under development:

- ➢ Pancreas probe, diameter **15 mm**
  - Clamped on Fujinon EG-530UR2
- ➢ Prostate probe, diameter **23 mm**
  - Clamped on Hitachi EUP-U533

PET detector design: endoscopic probe

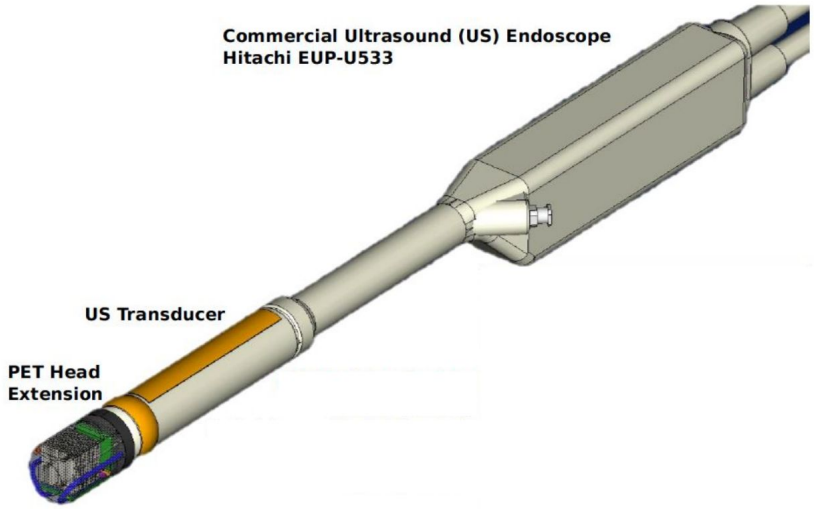

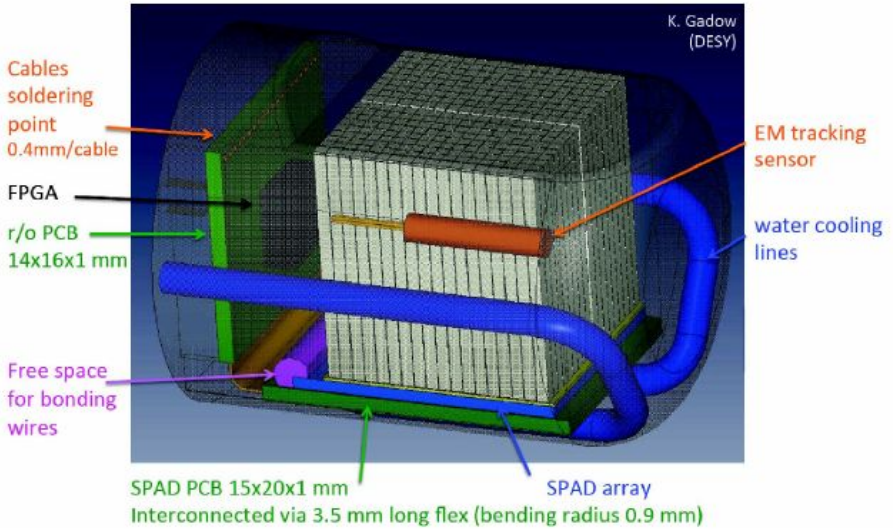

- **Two different versions** under development:
  - Pancreas probe, diameter **15 mm**
    - Clamped on Fujinon EG-530UR2
  - Prostate probe, diameter **23 mm**
    - Clamped on Hitachi EUP-U533
- **Scintillators**: 1 (pancreas) or 2 (prostate) arrays of **9x18 LYSO:Ce**
  - Individual crystal size **0.71x0.71x15**(or 10) **mm^3**
  - Crystal pitch **800 μm**
  - Coating material: ESR by 3M

PET detector design: endoscopic probe

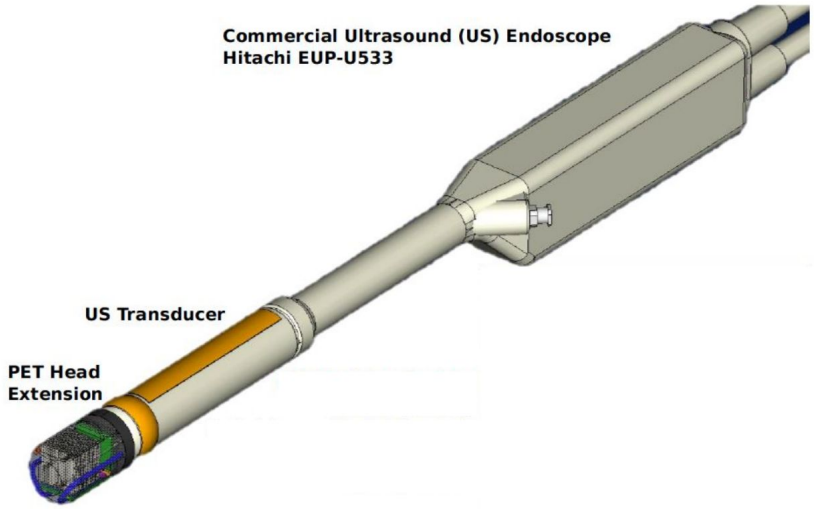

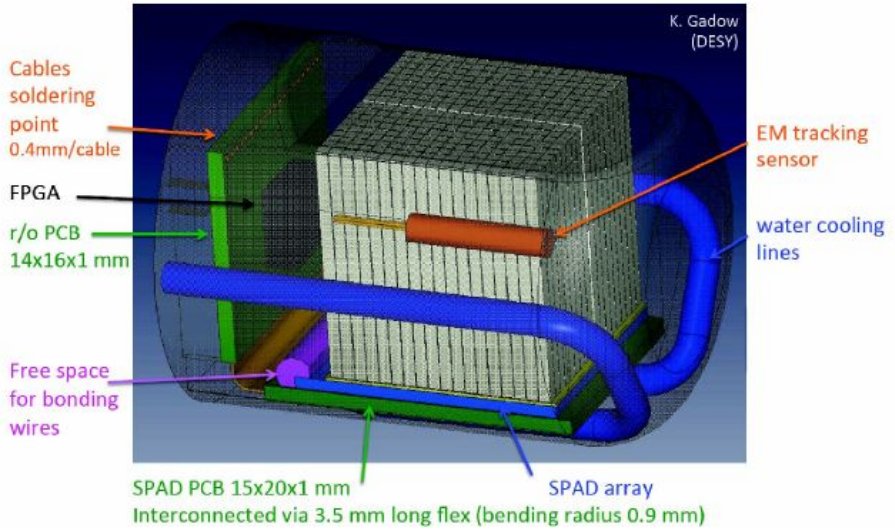

- ➔ **Two different versions** under development:
  - ➢ Pancreas probe, diameter **15 mm**
    - Clamped on Fujinon EG-530UR2
  - ➢ Prostate probe, diameter **23 mm**
    - Clamped on Hitachi EUP-U533
- ➔ **Scintillators**: 1 (pancreas) or 2 (prostate) arrays of **9x18 LYSO:Ce**
  - ➢ Individual crystal size **0.71x0.71x15**(or 10) **mm^3**
  - ➢ Crystal pitch **800 μm**
  - ➢ Coating material: ESR by 3M
- ➔ **Photo-detector**: custom **MD-SiPM** developed within the collaboration

PET detector design: endoscopic probe

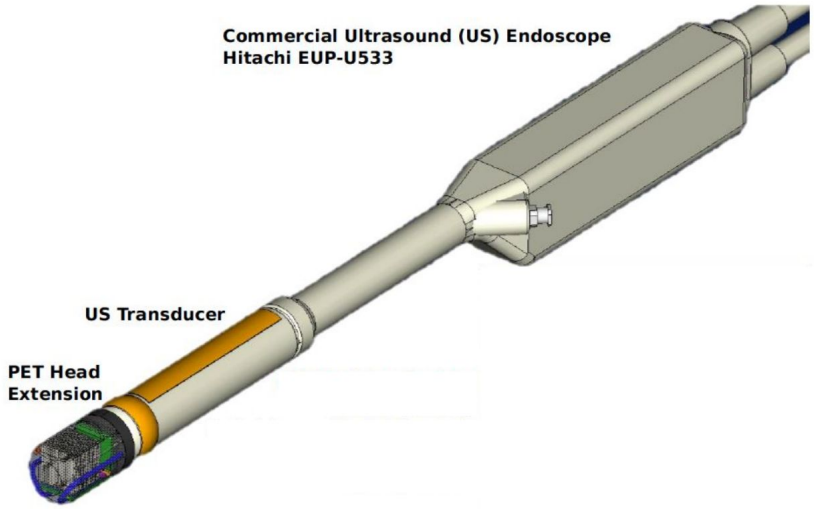

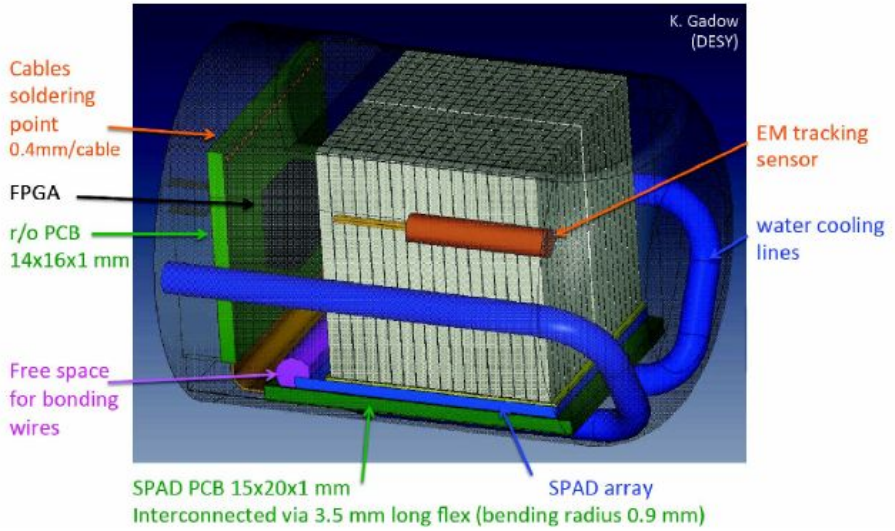

- **Two different versions** under development:
  - Pancreas probe, diameter **15 mm**
    - Clamped on Fujinon EG-530UR2
  - Prostate probe, diameter **23 mm**
    - Clamped on Hitachi EUP-U533
- **Scintillators**: 1 (pancreas) or 2 (prostate) arrays of **9x18 LYSO:Ce**
  - Individual crystal size **0.71x0.71x15**(or 10) **mm^3**
  - Crystal pitch **800 μm**
  - Coating material: ESR by 3M
- **Photo-detector**: custom **MD-SiPM** developed within the collaboration
- EM, and optical **tracking**, water **cooling**

Detector performance

PET detector performance: scintillators

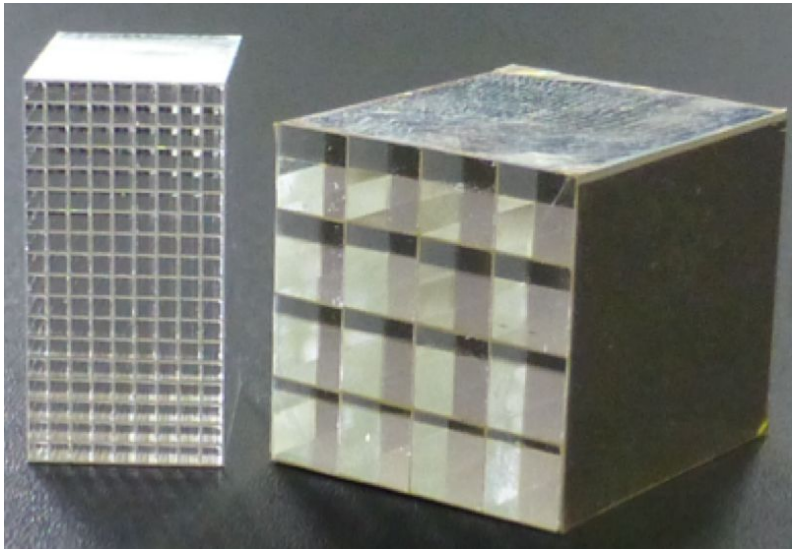

- ➔ **LYSO:Ce** polished scintillators, coating with ESR
- ➔ Required light output to reach 200ps = **20000-25000 Ph/MeV**
- ➔ 9x18 arrays of internal probes tested on standard PMTs (optical grease coupling)
  - ➢ Narrow sum photopeak ensure uniform light output within individual arrays
  - ➢ Average light output = **28000 +/- 1000 Ph/MeV**

PET detector performance: scintillators

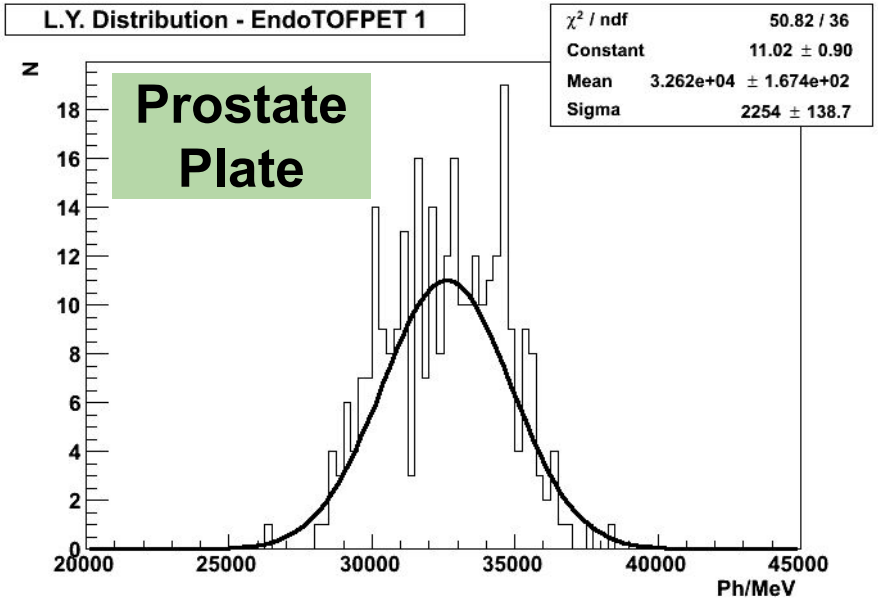

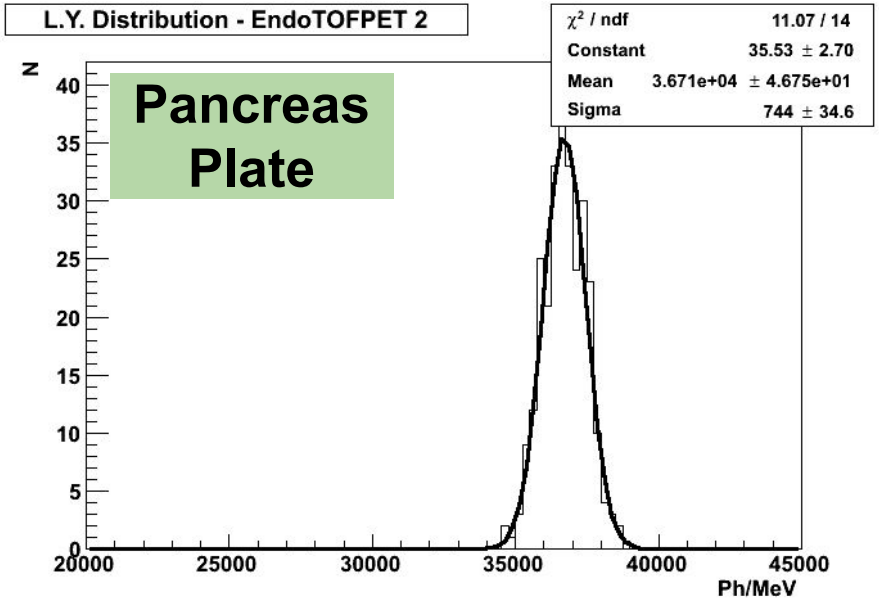

- **LYSO:Ce** polished scintillators, coating with ESR
- Required light output to reach 200ps = **20000-25000 Ph/MeV**
- 9x18 arrays of internal probes tested on standard PMTs (optical grease coupling)
  - Narrow sum photopeak ensure uniform light output within individual arrays
  - Average light output = **28000 +/- 1000 Ph/MeV**
- Characterization of 276(x2) arrays produced for external plates with **MiniACCOS**
  - 25 arrays per teflon plate
  - Motorized X-Y movements
  - Average light output (Prostate) = **32000 +/- 2000 Ph/MeV**
  - Average light output (Pancreas) = **37000 +/- 3000 Ph/MeV**

PET detector performance: MPPCs

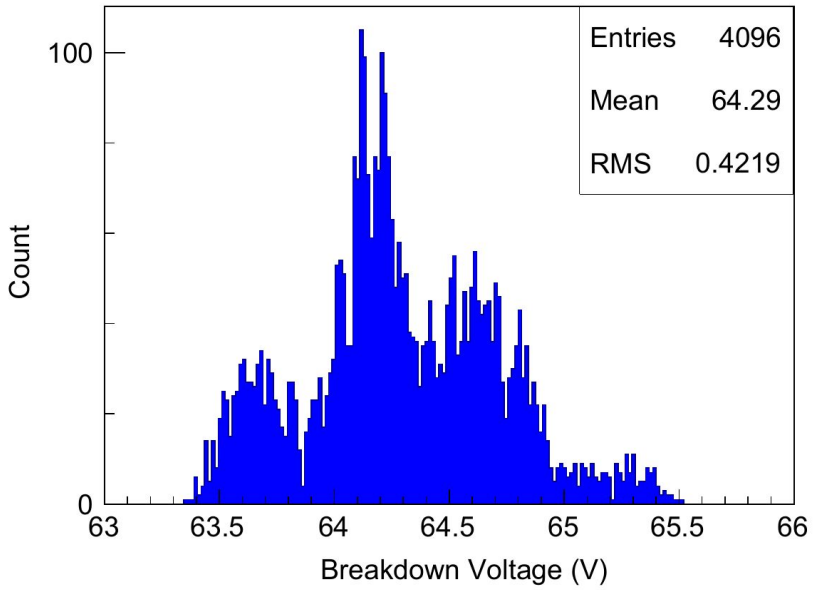

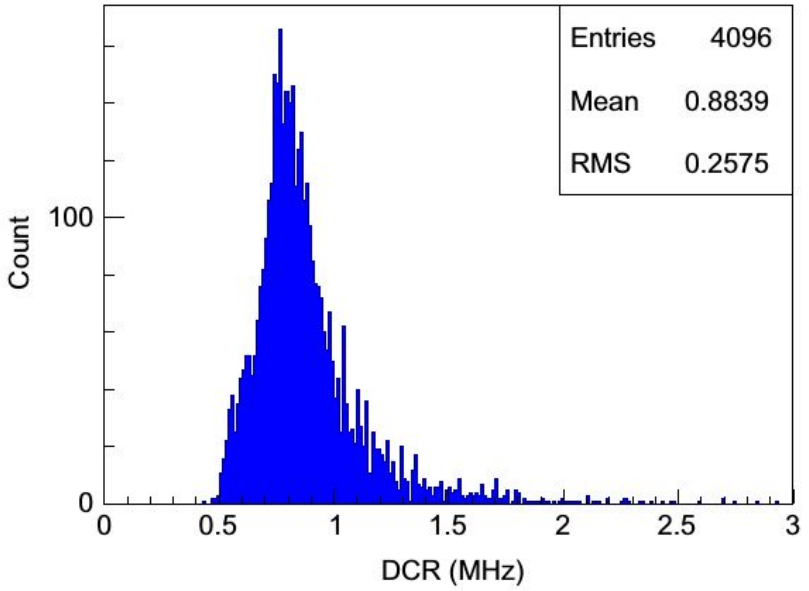

- ➔ Characterization of breakdown voltage (V_{bd}) with I-V curves
  - ➢ Measured with Keithley 2410 for each channel of the 256 MPPCs, at 19 °C
  - ➢ **Excellent homogeneity** within 16 channels of each array
  - ➢ MPPCs sorted on the bases of V_{bd} distribution (common bias for 4 MPPCs)
  - ➢ Operational voltage set to $\mathbf{V_{bd} + 2.5\ V}$
- ➔ Average Dark Count Rate (DCR) and Cross Talk
  - ➢ DCR measured as a function of the NINO amplifier/discriminator threshold
  - ➢ Average **DCR** at 19 °C = **0.88 MHz**
  - ➢ Cross Talk between SPADs measured as the ratio of DCR at 1.5 to 0.5 photoelectrons
  - ➢ Average **SPAD cross talk** at 19 °C = **41.4%**

PET detector performance: modules

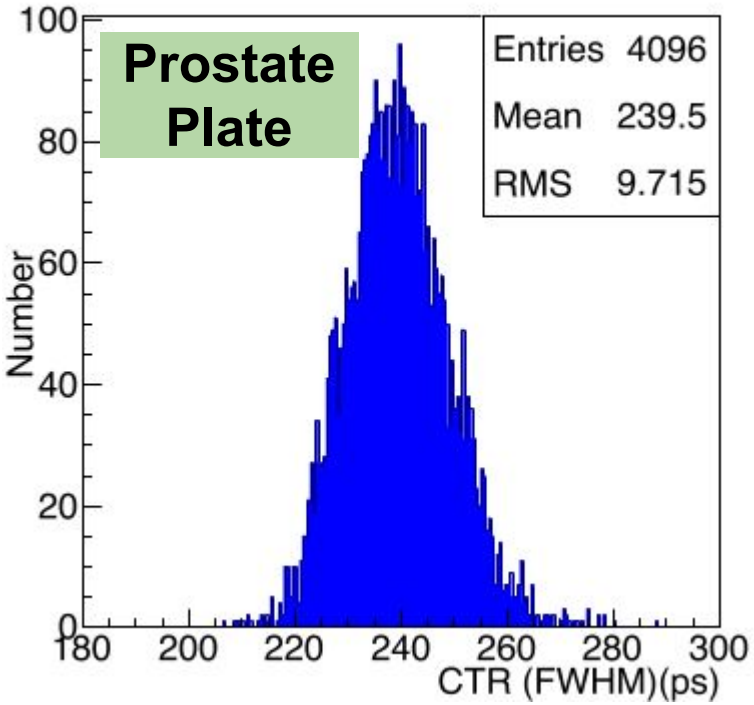

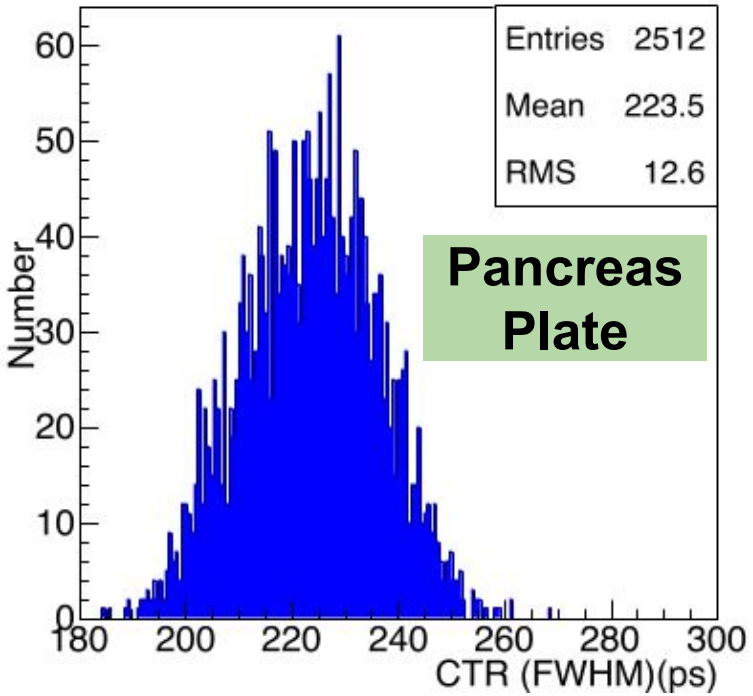

- Light Output of all modules determined as number of pixels fired
  - Module excited with ^{22}Na source
  - Current output integrated by QDC over 100 ns gate
  - Mean Light Output = 1876 +/- 100 pixels fired
  - Mean **Energy Resolution FWHM** = **12.8%**
- Coincidence Time Resolution (CTR)
  - Measured with NINO and HPTDC for each module against a reference module
  - Average prostate plate **CTR_{FWHM}** = **239.5 ps**
  - Average pancreas plate **CTR_{FWHM}** = **223.5 ps**

PET detector performance: ASICs

	STiC	TOFPET-ASIC
Jitter (at >5pC)	< 30 ps	< 25 ps
Input bias lin. range	0.7 V	0.5 V
TDC time bin width	50 ps	50 ps
Power consumption	19 mW/ch.	8 mW/ch
Output rate	160 MBit/s	160 MBit/s

➔ Two dedicated fast 64 channel ASICs developed: **StiC** and **TOFPET**

- ➢ Leading edge technique to get timing information
- ➢ Linearized Time-Over-Threshold method to provide energy information
- ➢ Low noise, low timing-jitter, low power consumption

PET detector performance: ASICs

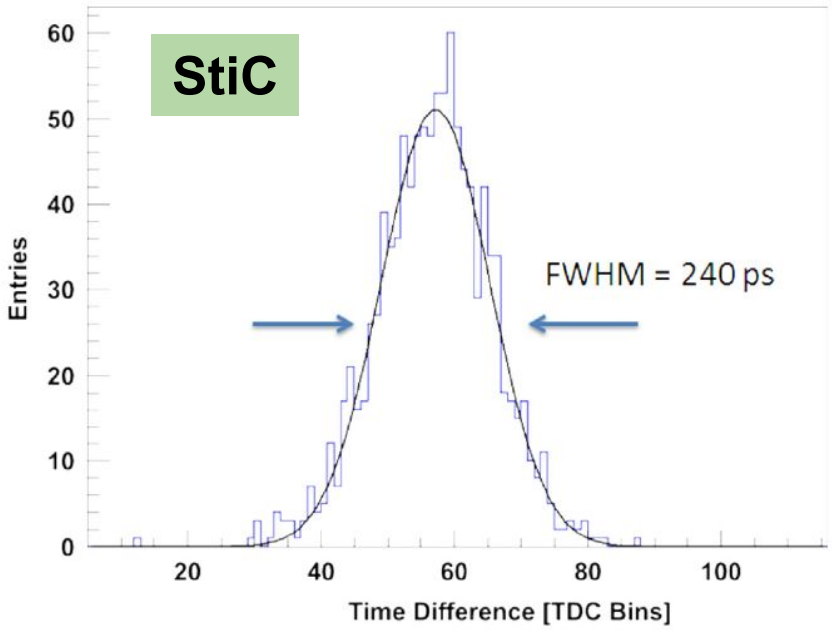

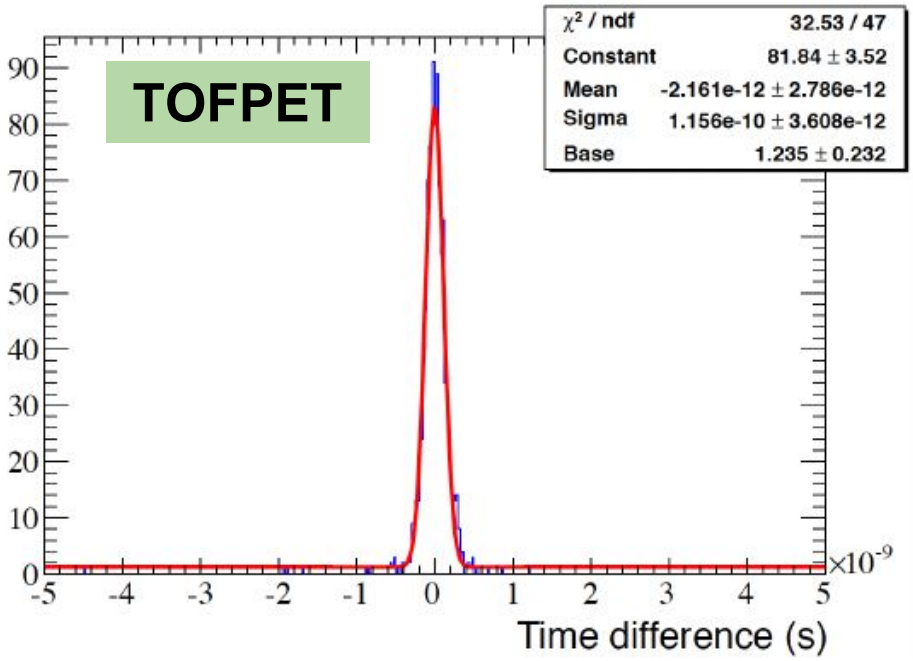

➔ Two dedicated fast 64 channel ASICs developed: **StiC** and **TOFPET**
- ➢ Leading edge technique to get timing information
- ➢ Linearized Time-Over-Threshold method to provide energy information
- ➢ Low noise, low timing-jitter, low power consumption

➔ **CTR** measured for both ASICs
- ➢ Single 3.1x3.1x15 mm^3 crystals coupled to 2 Hamamatsu MPPCs
- ➢ ^{22}Na source
- ➢ StiC average $\mathbf{CTR_{FWHM}}$ = **240 ps**
- ➢ TOFPET average $\mathbf{CTR_{FWHM}}$ = **270 ps**

Endoscopic probe: MD-SiPM

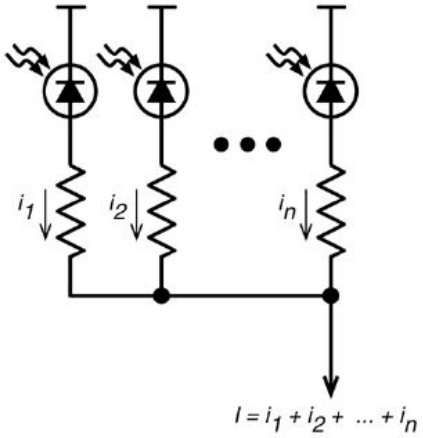

Analog SiPM

Endoscopic probe: MD-SiPM

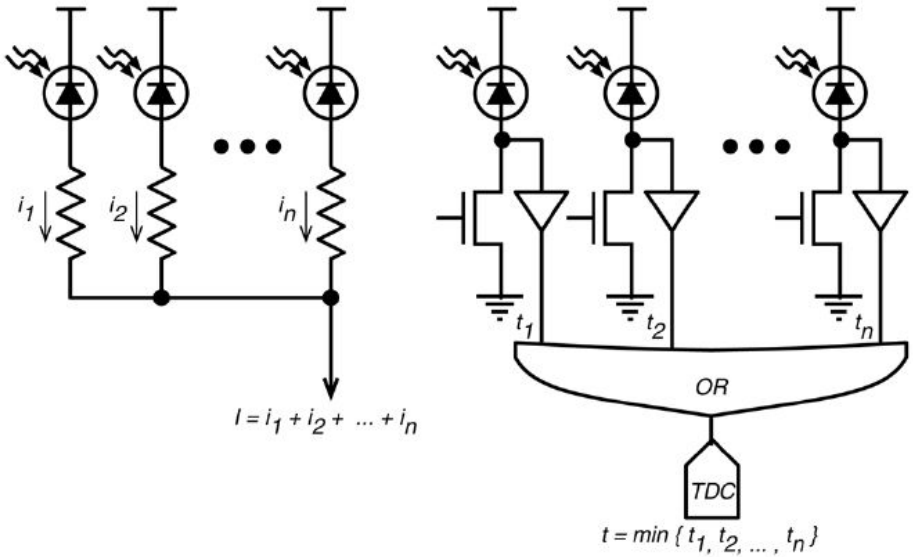

Analog SiPM

Conventional Digital SiPM

Endoscopic probe: MD-SiPM

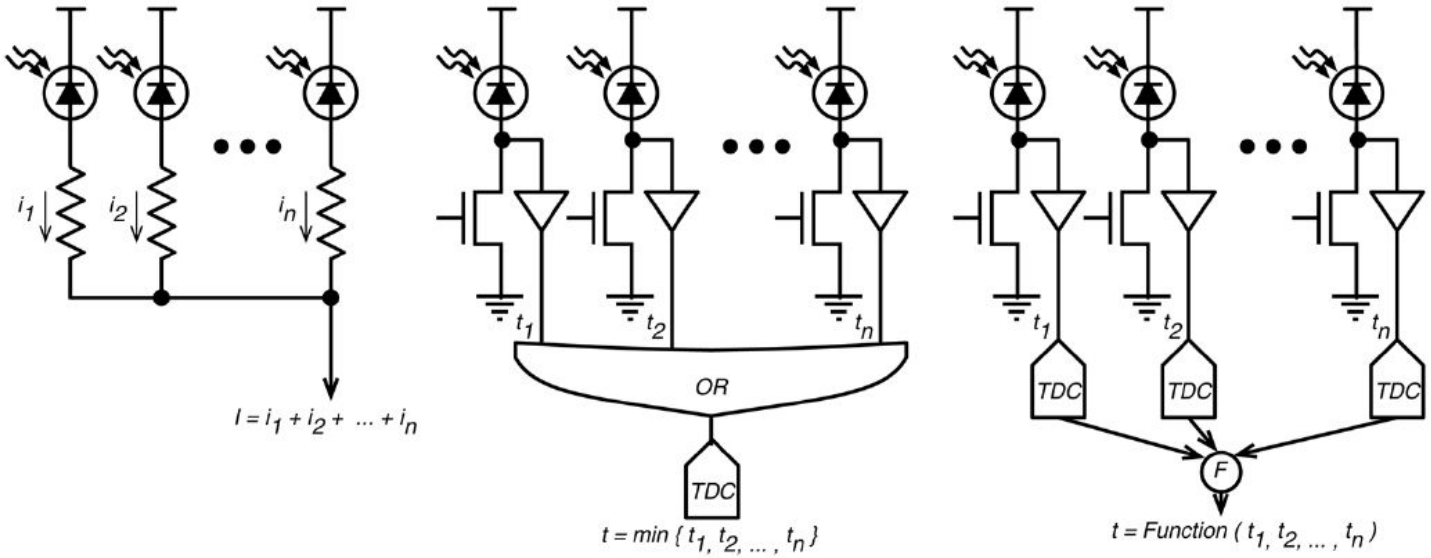

Analog SiPM

Conventional Digital SiPM

Fully digital SiPM

Endoscopic probe: MD-SiPM

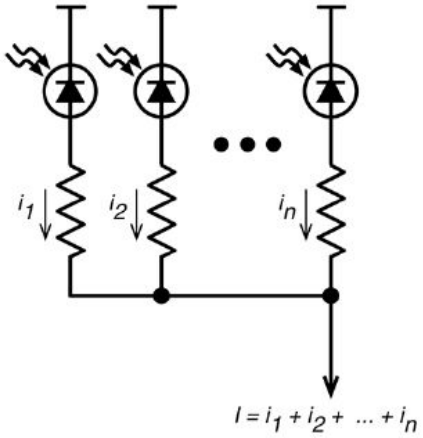

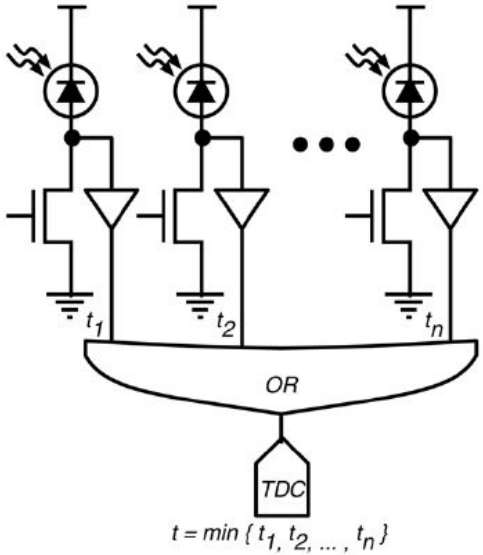

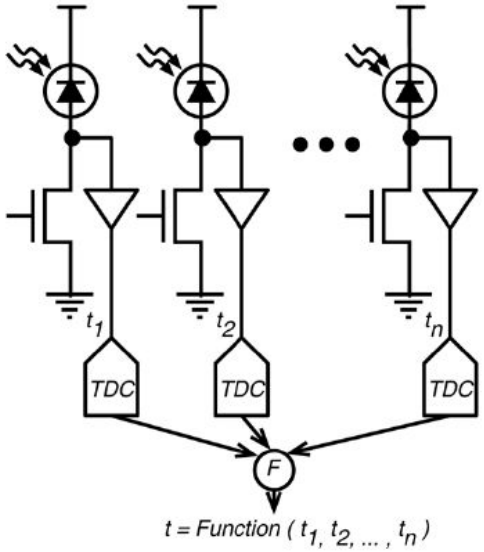

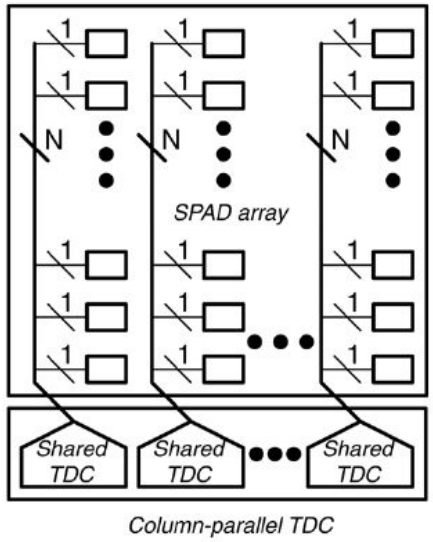

Analog SiPM

Conventional Digital SiPM

Fully digital SiPM

Multi Digital SiPM

Endoscopic probe: MD-SiPM

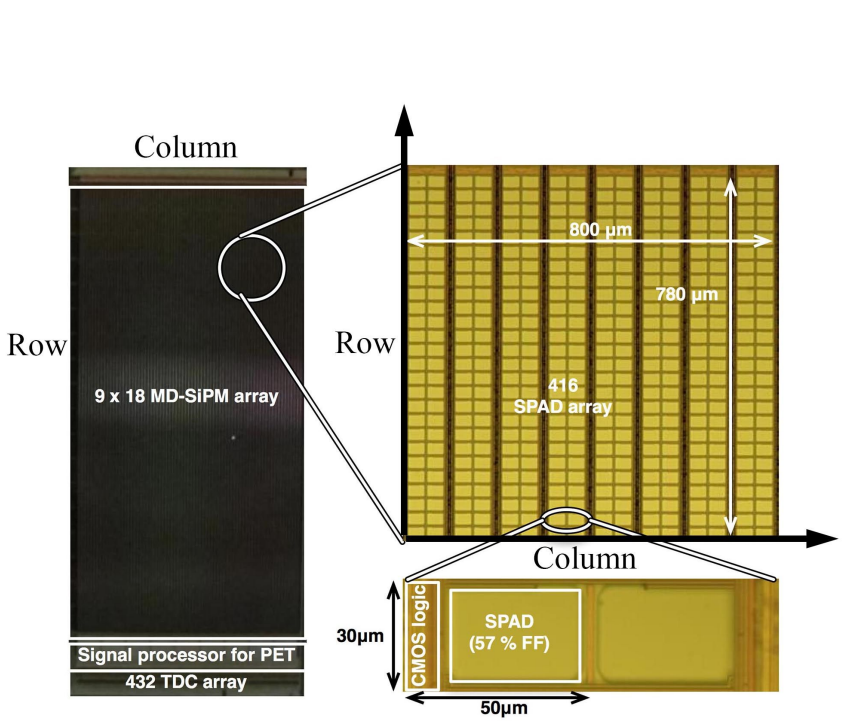

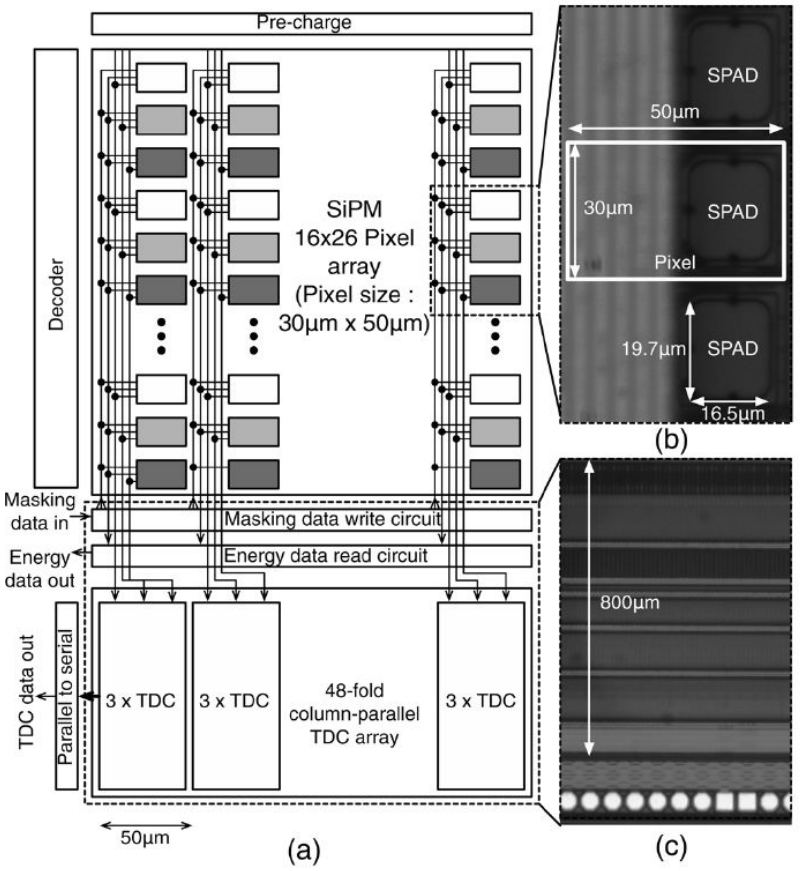

- ➔ Individual SPADs size **30x50 µm**, 57% fill factor
  - ➢ 1-bit counter per SPAD provides digital count of pixels fired
- ➔ 416 SPADs per MD-SiPM (16x26 array), size **780x800µm**
  - ➢ Pixel masking
- ➔ Array of **9x18 MD-SiPMs** matching the scintillator matrix
  - ➢ 432 column-parallel TDCs (48 per column)
  - ➢ Combining information of first 48 photons reaching **lower bound** of theoretically achievable CTR

Endoscopic probe: MD-SiPM

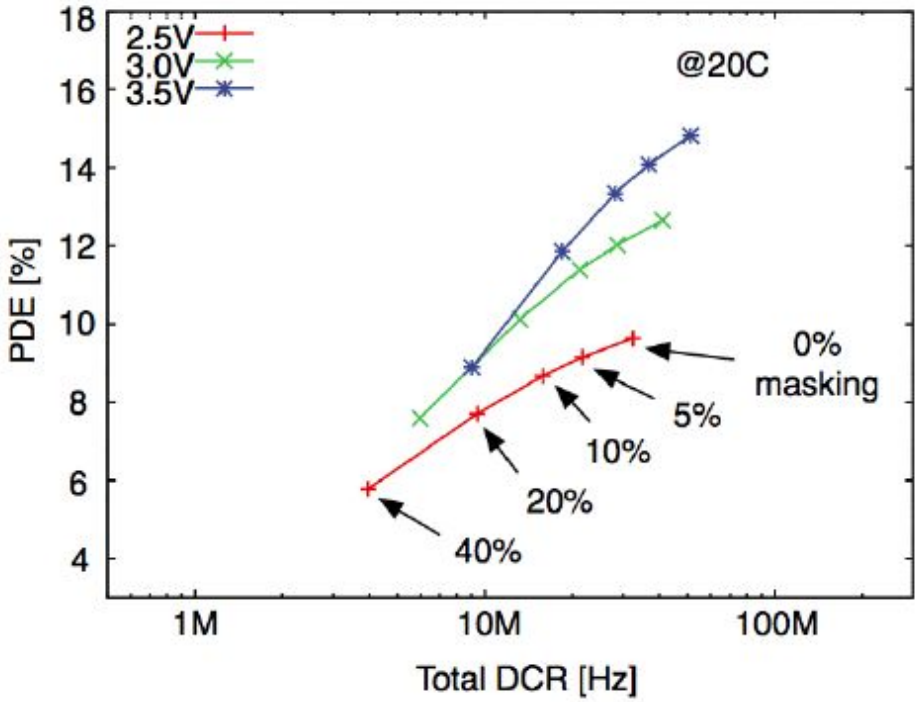

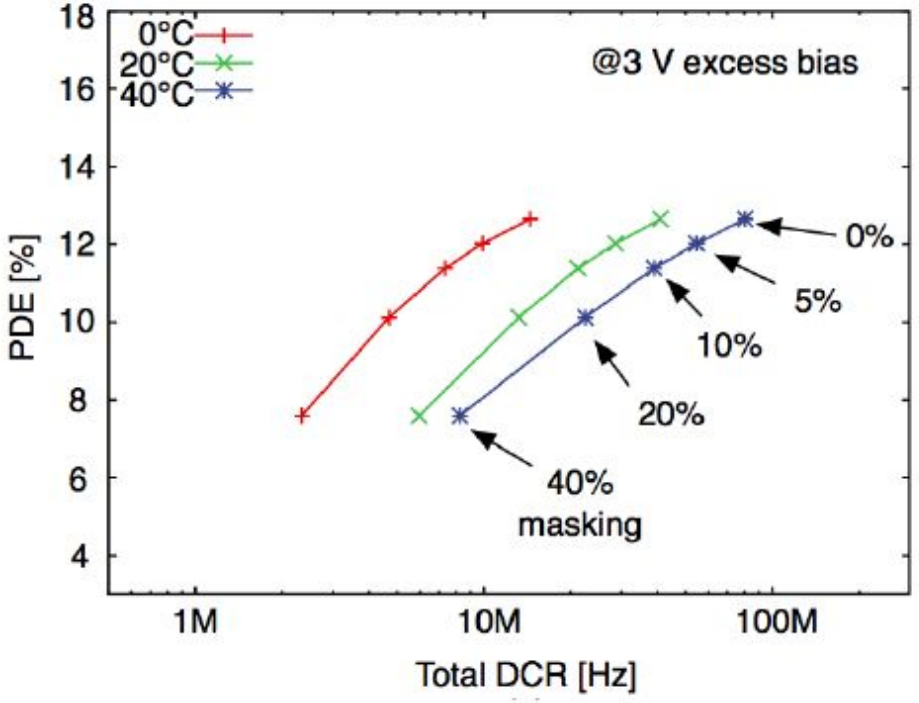

➔ DCR measured for different temperatures and bias voltages

- ➢ DCR 41 MHz at 20 °C and 3 V excess bias
- ➢ Can be reduced to 23 MHz with 10% masking
- ➢ PDE after masking about 12%

Endoscopic probe: MD-SiPM

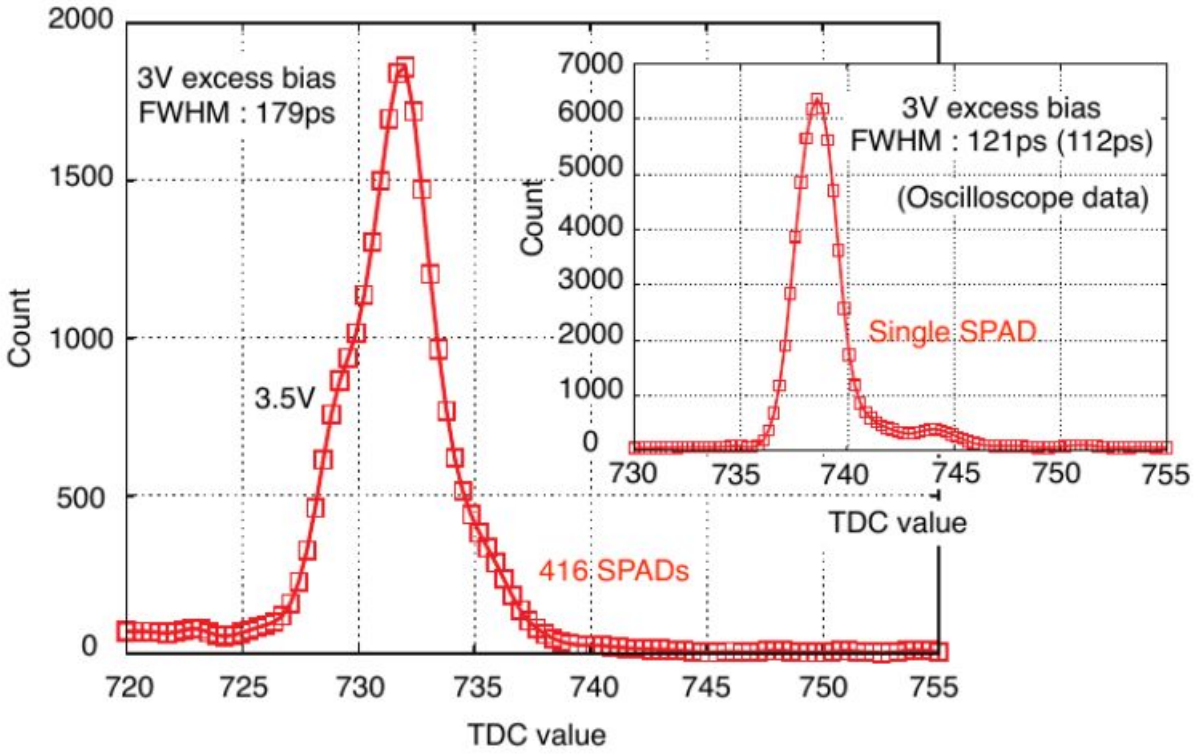

- ➔ DCR measured for different temperatures and bias voltages
  - ➢ DCR 41 MHz at 20 °C and 3 V excess bias
  - ➢ Can be reduced to 23 MHz with 10% masking
  - ➢ PDE after masking about 12%
- ➔ Single Photon Timing Resolution (SPTR) evaluated
  - ➢ Pulsed laser (250 mW, 405 nm, 40ps pulse width)
  - ➢ Internal TDCs (45 ps LSB)
  - ➢ $SPTR_{FWHM}$ measured in **121 ps** for single SPAD and **179 ps** for entire 16x26 array

Reconstruction Algorithm - Simulations

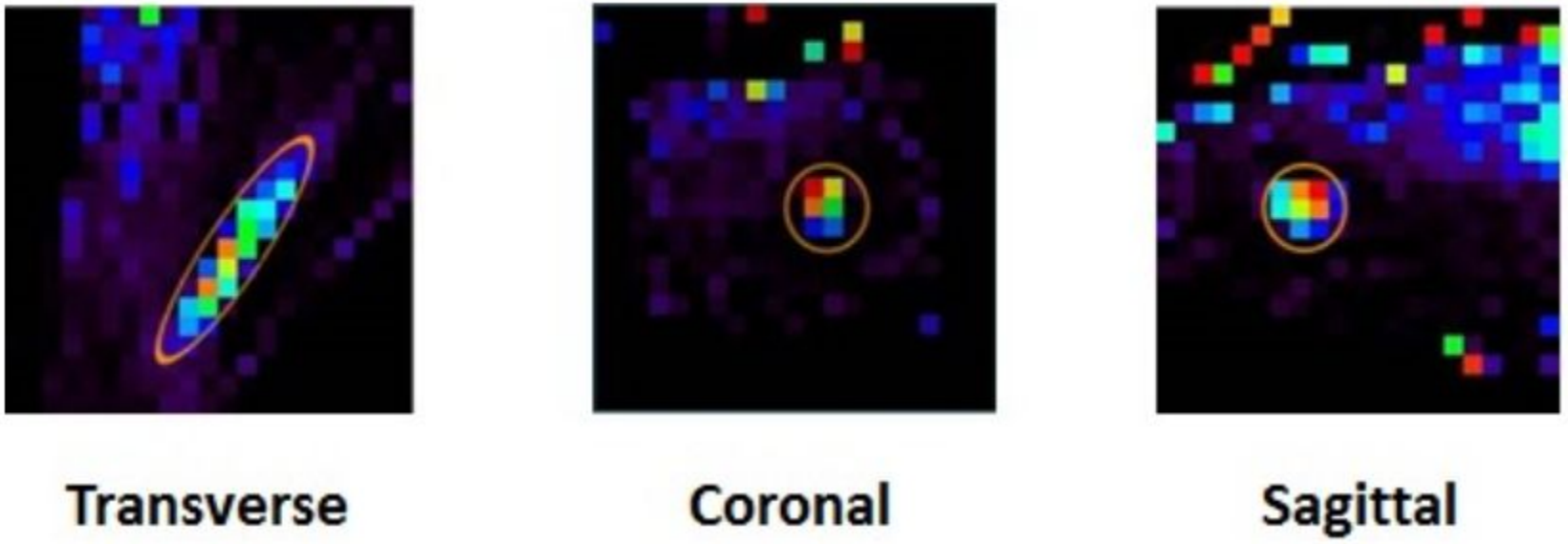

- ➔ Dedicated reconstruction algorithm developed within the collaboration
  - ➢ Iterative **histogram based ML-EM** reconstruction
  - ➢ Incorporates TOF information
  - ➢ Copes with detector asymmetry
  - ➢ Takes into account the limited rotation capabilities
  - ➢ Massive parallelization by GPU programming
- ➔ Expected performance tested on **simulated datasets**
  - ➢ Based on GAMOS toolkit
  - ➢ **1 mm resolution** within reach with **10 minutes** scan time

Commissioning and testing of first prototype

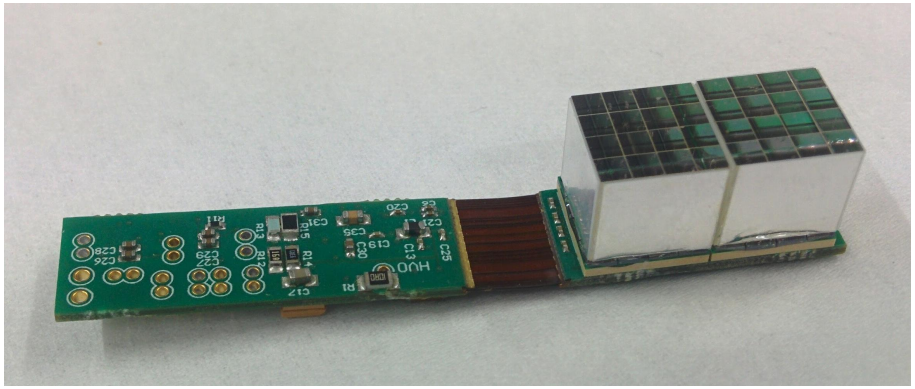

➔ **Provisional probe** with 2 MPPCs and 2 4x4 LYSO:Ce arrays (3.1x3.1x15 mm^3)

Commissioning and testing of first prototype

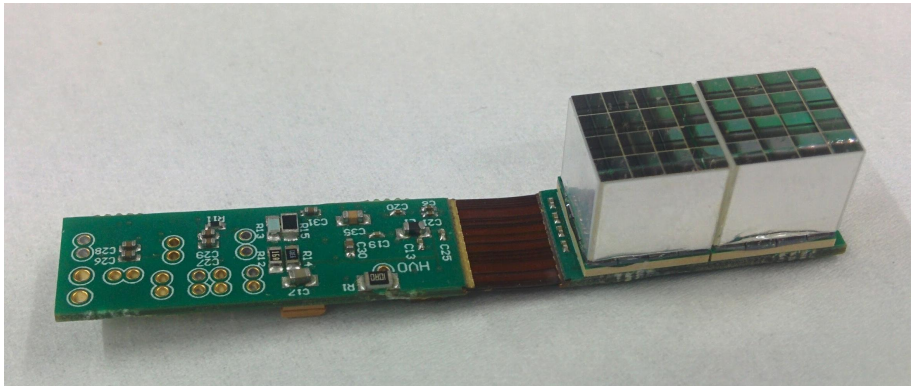

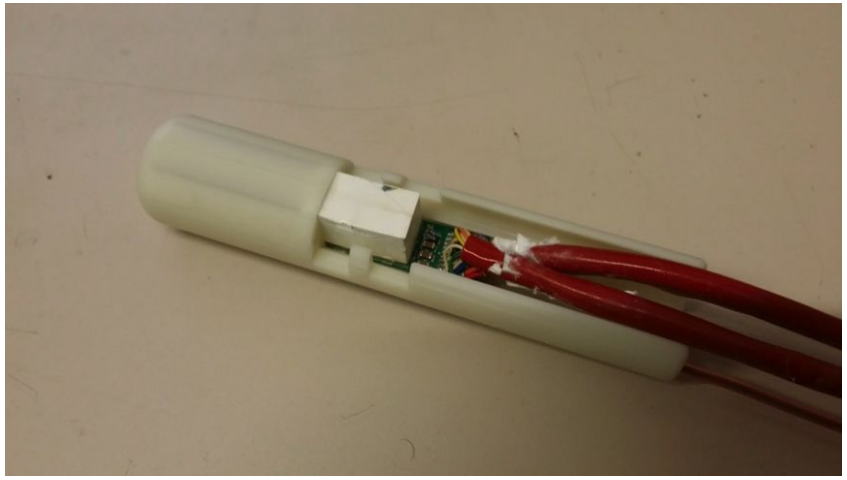

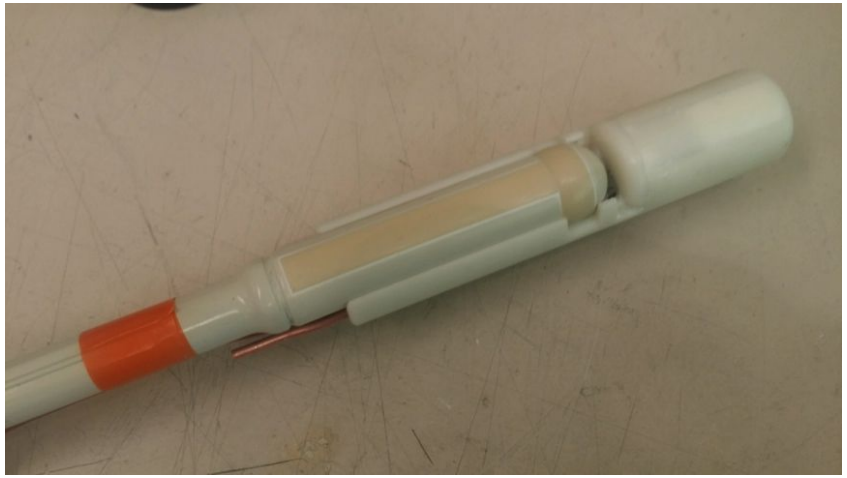

➔ **Provisional probe** with 2 MPPCs and 2 4x4 LYSO:Ce arrays (3.1x3.1x15 mm^3)

➔ Clamping on prostate US endoscope

Commissioning and testing of first prototype

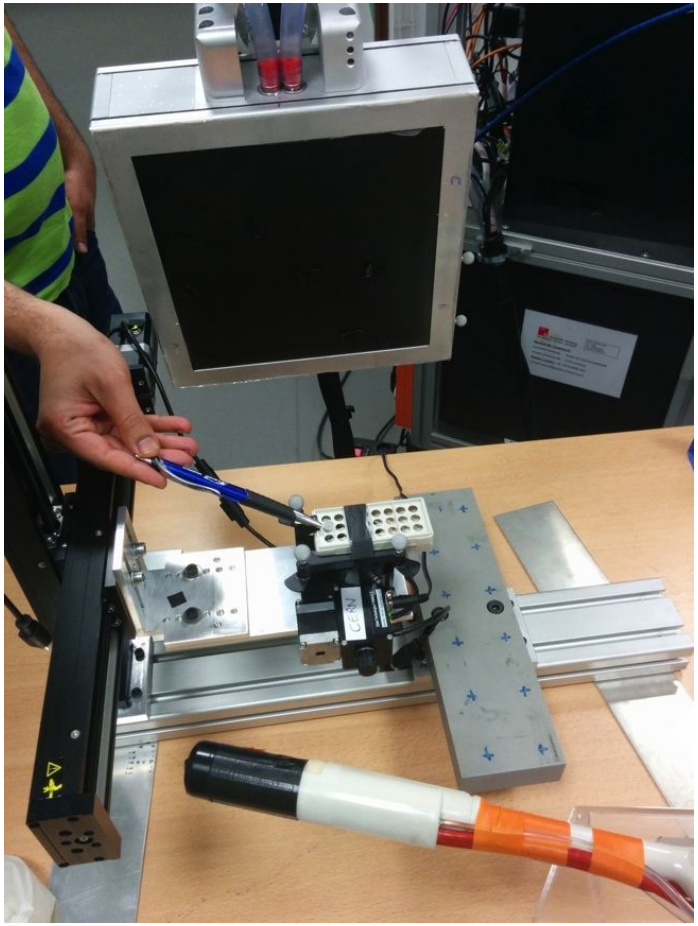

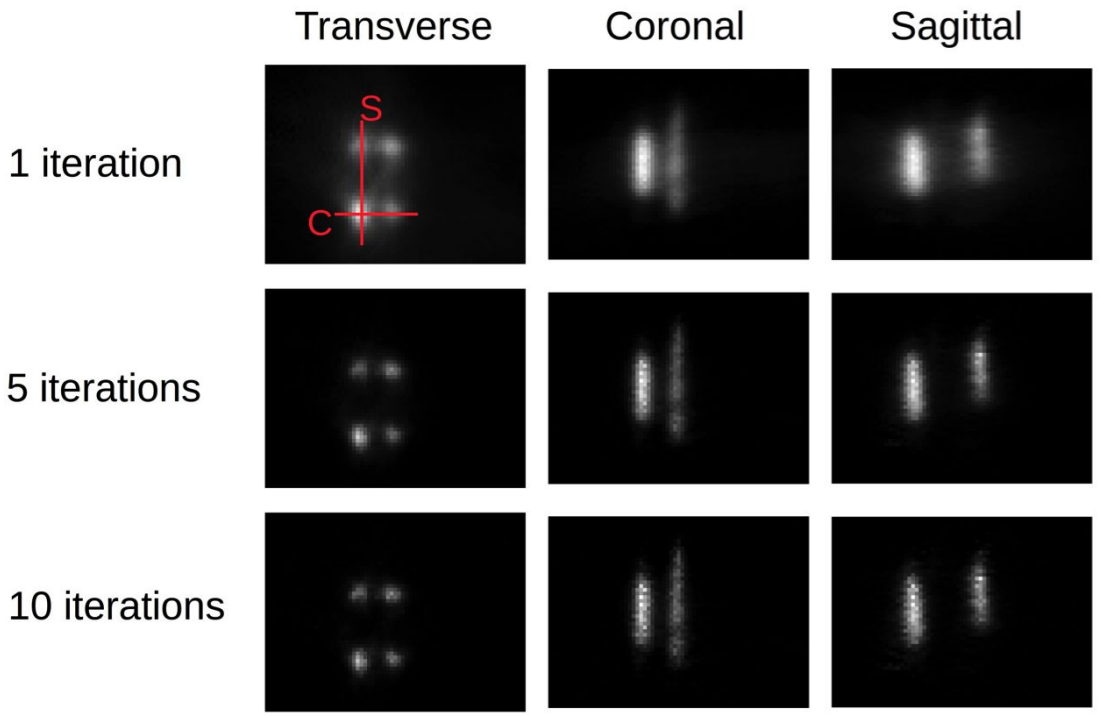

- ➔ **Provisional probe** with 2 MPPCs and 2 4x4 LYSO:Ce arrays (3.1x3.1x15 mm^3)
- ➔ Clamping on prostate US endoscope
- ➔ Preliminary images obtained at **CERIMED-Marseille** on cylinders filled with **FDG**

Development of new biomarkers

PANCREAS

	Non tumoral tissues	Tumoral tissues
Frozen tissue	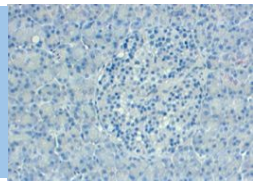 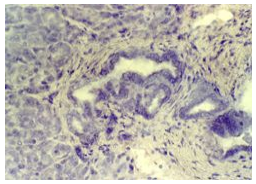	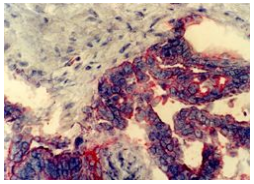 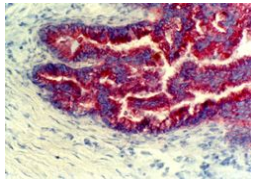
Formalin-fixed, paraffin-embedded tissues	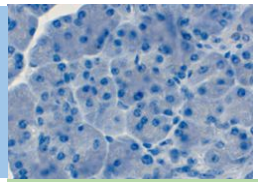 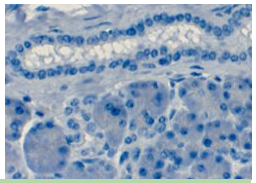	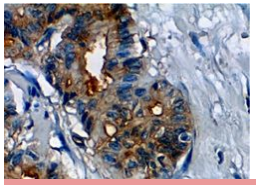 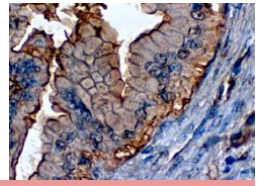

➔ Pancreas cancer: **mAb16D10**

- ➢ **Recognizes** human pancreatic tumor cells
- ➢ **Does not recognize** non-tumoral pancreatic tissue, other cancers or normal tissue
- ➢ **Therapeutic** properties: decreases tumor growth and mobility

Development of new biomarkers

PANCREAS

Frozen tissue

Formalin-fixed, paraffin-embedded tissues

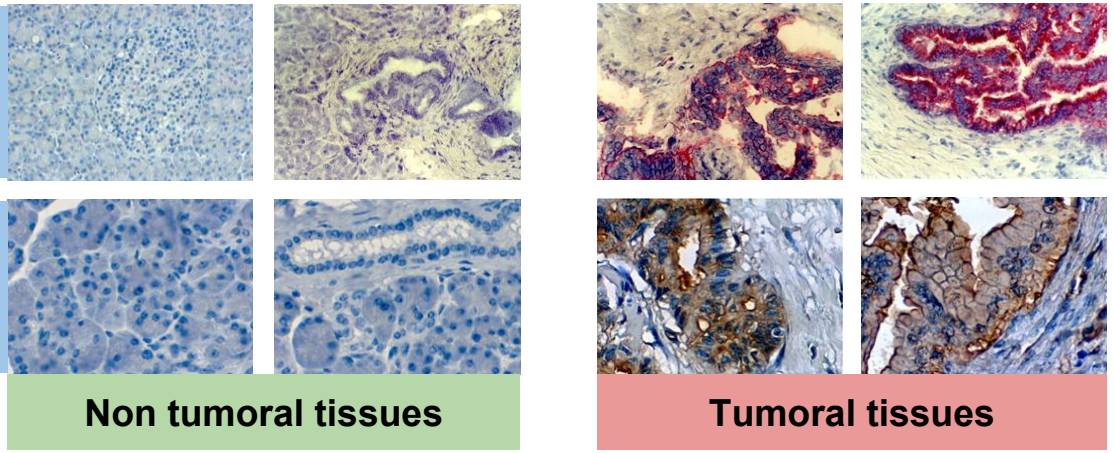

Non tumoral tissues | **Tumoral tissues**

PROSTATE

68Ga-PSMA PET/MR in patient with negative prostate biopsy

- ➔ Pancreas cancer: **mAb16D10**
  - ➢ **Recognizes** human pancreatic tumor cells
  - ➢ **Does not recognize** non-tumoral pancreatic tissue, other cancers or normal tissue
  - ➢ **Therapeutic** properties: decreases tumor growth and mobility
- ➔ Prostate cancer: **^{68}Ga-PSMA**
  - ➢ **Enzyme** expressed by prostate epithelial cells
  - ➢ **More specific** as compared to standard ^{18}F and ^{11}C tracers

Lessons learned

➔ Several positive **by-products** of research

- ➢ Investigation of new crystals (**garnets**, …)
- ➢ Study on diffractive optics and **photonic crystals**
- ➢ Necessity to focus on new light sources for the 10ps frontier (**nanocrystal**, …)
- ➢ **TOFPET ASIC** selected for the CMS detector upgrade @LHC
- ➢ First stage of development of the **MD-SiPM**

Lessons learned

➔ Several positive **by-products** of research
- ➢ Investigation of new crystals (**garnets**, …)
- ➢ Study on diffractive optics and **photonic crystals**
- ➢ Necessity to focus on new light sources for the 10ps frontier (**nanocrystal**, …)
- ➢ **TOFPET ASIC** selected for the CMS detector upgrade @LHC
- ➢ First stage of development of the **MD-SiPM**

➔ Need to rethink (or integrate) the way EU is **financing** frontier projects
- ➢ Very ambitious projects cannot bring to a complete system in the turn of 5 years
- ➢ New funding schemes are in fact under study by the EU Commission

Conclusions

➔ The **EndoTOFPET-US** collaboration is developing a multi-modal PET-US scanner for early detection of prostate and pancreas cancer

Conclusions

➔ The **EndoTOFPET-US** collaboration is developing a multi-modal PET-US scanner for early detection of prostate and pancreas cancer

➔ The PET scanner design aims to **1-2 mm** spatial resolution and **200 ps** FWHM CTR

- ➢ **Early diagnosis**, via spatial resolution and SNR and NEC improvement from TOF
- ➢ Tool for development of new **biomarkers**
- ➢ Research to develop this scanner will be instrumental in the **effort towards the "10 ps PET"** (e.g. MD-SiPM, fast ASICs, scintillators, etc.)

Conclusions

- The **EndoTOFPET-US** collaboration is developing a multi-modal PET-US scanner for early detection of prostate and pancreas cancer

- The PET scanner design aims to **1-2 mm** spatial resolution and **200 ps** FWHM CTR
  - **Early diagnosis**, via spatial resolution and SNR and NEC improvement from TOF
  - Tool for development of new **biomarkers**
  - Research to develop this scanner will be instrumental in the **effort towards the "10 ps PET"** (e.g. MD-SiPM, fast ASICs, scintillators, etc.)

- Performance of single components evaluated, design targets **within reach**

- Two external detectors assembled, **first tests** with provisional internal probe

- Several lessons learned

Thank you for your attention!

Thanks to all the collaborators of
EndoTOFPET-US and PicoSEC-MCNet

This project have been partially funded by from the European Union 7th Framework Program (FP7/ 2007-2013) under Grant Agreement No. 256984 (EndoTOFPET-US) and is supported by a Marie Curie Early Initial Training Network Fellowship of the European Community's Seventh Framework Programme under contract number (PITN-GA-2011-289355-PicoSEC-MCNet)